

U.S. DEPARTMENT OF COMMERCE
National Technical Information Service

AD-A026 464

TEMPERATURE COMPENSATED PIEZOELECTRIC MATERIALS

PENNSYLVANIA STATE UNIVERSITY

PREPARED FOR
ROME AIR DEVELOPMENT CENTER

JUNE 1976

194086

RADC-TR-76-184
Interim Technical Report
June 1976

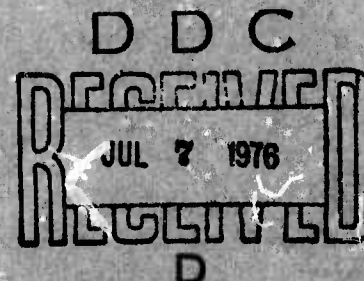


**TEMPERATURE COMPENSATED
PIEZOELECTRIC MATERIALS**

**Materials Research Laboratory
The Pennsylvania State University**

Approved for public release; distribution unlimited.

Sponsored by
Defense Advanced Research Projects Agency
ARPA Order No. 2826



**ROME AIR DEVELOPMENT CENTER
AIR FORCE SYSTEMS COMMAND
GRIFFISS AIR FORCE BASE, NEW YORK 13441**

REPRODUCED BY
**NATIONAL TECHNICAL
INFORMATION SERVICE**
U.S. DEPARTMENT OF COMMERCE
SPRINGFIELD, VA. 22161

ADA 026 464

REPORT DOCUMENTATION PAGE		READ INSTRUCTIONS BEFORE COMPLETING FORM
1. REPORT NUMBER RADC-TR-76-184	2. GOVT ACCESSION NO.	3. RECIPIENT'S CATALOG NUMBER
4. TITLE (and Subtitle) TEMPERATURE COMPENSATED PIEZOELECTRIC MATERIALS		5. TYPE OF REPORT & PERIOD COVERED Interim 1 July 75 - 31 December 75
		6. PERFORMING ORG. REPORT NUMBER Semi Tech Report No. 2
7. AUTHOR(s) G. R. Barsch K. E. Spear		8. CONTRACT OR GRANT NUMBER(s) F 19628-75-C-0085
9. PERFORMING ORGANIZATION NAME AND ADDRESS Materials Research Laboratory The Pennsylvania State University University Park, Pennsylvania 16802		10. PROGRAM ELEMENT, PROJECT, TASK AREA & WORK UNIT NUMBERS PE 61101F 2826
11. CONTROLLING OFFICE NAME AND ADDRESS Defense Advanced Projects Agency 1400 Wilson Blvd. Arlington, VA 22209		12. REPORT DATE June 1976
		13. NUMBER OF PAGES 55
14. MONITORING AGENCY NAME & ADDRESS (if different from Controlling Office) Deputy for Electronic Technology (RADC/ETEM) Hanscom AFB MA 01731 Contract Monitor, Paul H. Carr (ETEM)		15. SECURITY CLASS. (of this report) Unclassified
		15a. DECLASSIFICATION/DOWNGRADING SCHEDULE
16. DISTRIBUTION STATEMENT (of this Report) APPROVED FOR PUBLIC RELEASE; DISTRIBUTION UNLIMITED		
17. DISTRIBUTION STATEMENT (of the abstract entered in Block 20, if different from Report)		
18. SUPPLEMENTARY NOTES This work is sponsored by the Defense Advanced Projects Agency; ARPA Order No. 2826.		
19. KEY WORDS (Continue on reverse side if necessary and identify by block number) Crystal Growth; Ultrasonics; Elastic Constants; Thermoelastic Constants; Piezoelectric Constants; Temperature Compensated Materials; Lithium Silicate; Fresnoite; Lead Potassium Niobate.		
20. ABSTRACT (Continue on reverse side if necessary and identify by block number) In order to search for new temperature compensated materials for surface acoustic wave (SAW) devices with low ultrasonic attenuation and high electro- mechanical coupling, the following experimental and theoretical investigations were carried out: (1) Extensive crystal growth investigations were carried out for		

Li_2SiO_3 , $\text{Ba}_2\text{Si}_2\text{TiO}_8$, and $\text{Pb}_2\text{KNb}_5\text{O}_{15}$, using both Bridgman and Czochralski methods. For the two first mentioned materials, polycrystalline specimens were obtained so far, and for $\text{Pb}_2\text{KNb}_5\text{O}_{15}$ several single crystal pieces barely large enough for property measurements were obtained.

(ii) The on-diagonal elastic constants c_{11} , c_{22} , c_{33} , c_{44} and c_{55} and their temperature coefficients have been measured for $\text{Pb}_2\text{KNb}_5\text{O}_{15}$. The temperature coefficient of c_{11} is positive, indicating that temperature compensated cuts should exist for this material.

(iii) The theoretical equations required for the experimental determination of the complete set of piezoelectric constants from X-ray measurements have been derived. For this purpose the expression for the quantity $(\partial\theta/\partial E)$, where θ denotes the Bragg angle and E the magnitude of an applied electric field is calculated as a function of the field direction and the reflecting lattice plane normal. For all 20 crystal classes exhibiting the piezoelectric effect explicit expressions are given for the longitudinal and transverse piezoelectric effect, corresponding to parallel-field and perpendicular-field reflection, respectively.

SEARCHED	<input checked="" type="checkbox"/>
SERIALIZED	<input type="checkbox"/>
INDEXED	<input type="checkbox"/>
FILED	<input type="checkbox"/>
JUL 7 1978	
FBI - NEW YORK	
A	

DDC
RECEIVED
JUL 7 1978
RECEIVED
D

TEMPERATURE COMPENSATED PIEZOELECTRIC MATERIALS

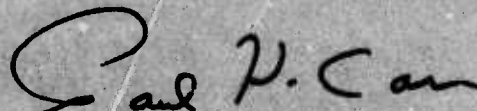
Contractor: The Pennsylvania State University
Contract Number: F19628-75-C-0085
Effective Date of Contract: 31 January 1975
Contract Expiration Date: 31 March 1977
Program Code Number: 5D10
Period of Work Covered: 1 July 75 - 31 December 75
Principal Investigators: G. R. Barsch, (814) 865-1657
K. E. Spear, (814) 865-1198
Project Engineer: Paul H. Carr (617) 861-2527

The views and conclusions contained in this document are those of the authors and should not be interpreted as necessarily representing the official policies, either expressed or implied, of the Defense Advanced Research Projects Agency or the U.S. Government.

This report has been reviewed by the ESD/RADC Information Office (OI) and is releasable to the National Technical Information Service (NTIS). At NTIS it will be releasable to the general public including foreign nations.

This report has been reviewed and is approved for publication.

APPROVED:



PAUL H. CARR
Project Engineer

11a

Acknowledgments

The authors would like to thank their collaborators for their participation in this work: Dr. L. Drafall for most of the crystal growth work, and Mr. W. B. Regnault for the crystal growth and the elastic constant measurements on lead potassium niobate.

TEMPERATURE COMPENSATED PIEZOELECTRIC MATERIALS

TABLE OF CONTENTS

	Page
Report Documentation Page and Abstract	1
Acknowledgments	iii
1. Technical Summary	1
1.1 Technical Problem	1
1.2 Methodological Approach	1
1.3 Technical Results	1
1.3.1 Crystal Growth	1
1.3.2 Measurement of Elastic, Thermoelastic, Piezoelectric and Dielectric Properties	2
1.4 DoD Implications	3
1.5 Implications and Further Research	3
1.6 Special Comments	3
2. Crystal Growth Results	4
2.1 Lithium Silicate	4
2.2 Fresnoite	5
2.3 Lead Potassium Niobate	6
3. X-Ray Determination of Piezoelectric Constants	6
3.1 Introduction	6
3.2 Theoretical Derivation	7
3.3 Application to Piezoelectric Crystal Classes	11
3.4 Specimen Orientation	29
3.5 Discussion of Tables 1 to 6	31
3.6 Numerical Example	33
4. Elastic and Thermoelastic Properties of Lead Potassium Niobate	41
5. References	47

1. Technical Summary

1.1 Technical Problem

The objective of the research of this contract is to find temperature compensated materials for use in surface acoustic wave (SAW) signal processing devices, i.e. materials with large electromechanical coupling, low ultrasonic attenuation and a vanishingly small temperature coefficient of the delay time. The electromechanical coupling factor should be substantially larger than for α -quartz, which is presently used in temperature compensated SAW devices.

1.2 Methodological Approach

The research consists of: (A) both exploratory and systematic crystal growth studies on a variety of materials which are expected to be temperature compensated for bulk waves and which have been selected earlier under AFCRL Contract F19628-73-C-108 on the basis of certain heuristic criteria (Barsch and Newnham, 1975), and (B) measurements of the single crystal elastic and thermo-elastic properties of the above grown crystals to determine whether they possess temperature compensated crystallographic directions for bulk waves, and measurements of their piezoelectric and dielectric constants and their corresponding temperature coefficients to check the suitability of these materials for surface wave device applications.

1.3 Technical Results

1.3.1 Crystal Growth

A. Crystal Growth: The crystal growth effort centered on Li_2SiO_3 , $\text{Ba}_2\text{Si}_2\text{TiO}_8$, and $\text{Pb}_2\text{KNb}_5\text{O}_{15}$. Both Bridgman and Czochralski crystal growth experiments were performed on Li_2SiO_3 , but the boules obtained were polycrystalline. The high temperature behavior of this phase was examined by DTA and high temperature x-ray techniques and indicated no major phase changes between room temperature and the melting point of Li_2SiO_3 . Various shielding

arrangements and temperature stability of the growth system were examined to determine their effects on the quality of the boules. Boules of $\text{Ba}_2\text{Si}_2\text{TiO}_8$ were pulled both from stoichiometric melts and from TiO_2 -rich melts. However, good quality crystals were not obtained in either case. The cracking problem in pulled $\text{Pb}_2\text{KNb}_5\text{O}_{15}$ crystals persisted, but was reduced by varying the lead content of the melt and decreasing the diameter of the boules. Several single crystal pieces barely large enough for measurements were obtained.

1.3.2 Measurement of Elastic, Thermoelastic, Piezoelectric and Dielectric Properties

The theoretical equations required for the experimental determination of the complete set of piezoelectric constants from X-ray measurements have been derived. For this purpose the expression for the quantity $(\partial\theta/\partial E)$, where θ denotes the Bragg angle and E the magnitude of an applied electric field is calculated as a function of the field direction and the reflecting lattice plane normal. For all 20 crystal classes exhibiting the piezoelectric effect explicit expressions are given for the longitudinal and transverse piezoelectric effect, corresponding to parallel-field and perpendicular-field reflection, respectively. For the 19 piezoelectric classes of the monoclinic, orthorhombic, tetragonal, trigonal, hexagonal and cubic systems explicit expressions for $(\partial\theta/\partial E)$ in terms of the Miller indices of the reflecting planes are given for the simplest crystal cuts with respect to the symmetry elements present.

The on-diagonal elastic constants c_{11} , c_{22} , c_{33} , c_{44} and c_{66} , and their temperature coefficients have been measured ultrasonically for lead potassium niobate, $\text{Pb}_2\text{KNb}_5\text{O}_{15}$. The elastic constant values differ considerably from results given by Yamada. The temperature coefficient of the longitudinal modulus c_{33} is found to be positive, substantiating earlier indications that lead potassium niobate should have temperature compensated cuts and therefore could be a superior substitute for α -quartz in SAW devices.

1.4 DoD Implications

For one of the materials investigated, lead potassium niobate, one may expect the existence of temperature compensated cuts for bulk and surface waves, with substantially larger electromechanical coupling than for α -quartz. Thus by replacing quartz as a substrate material in surface acoustic wave (SAW) devices by lead potassium niobate insertion losses can be reduced and the operating frequency and/or bandwidth can be increased. In this manner the efficiency, reliability and capability of military communications and Radar systems utilizing SAW signal processing devices, such as multichannel communications, secure anti-jam communications for satellites, miniature avionics and electromagnetic counter measures, can be improved.

1.5 Implications and Further Research

It has been demonstrated that the search for new temperature compensated materials with properties superior to those of α -quartz through the approach used under the present contract can be successful. One may therefore hope that a continued systematic search for new temperature compensated materials under the present contract may, even with the low funding level, eventually lead to the discovery of additional, perhaps even more suitable, materials. To this end continued crystal growth efforts are required to obtain suitable single crystals for the physical property measurements, which are necessary to assess the use of a given material for SAW device applications.

1.6 Special Comments

No special comments are offered at this time.

2. Crystal Growth Results

2.1 Lithium Silicate, Li_2SiO_3

Polycrystalline starting material of this phase was synthesized at 900°C from Li_2CO_3 and SiO_2 . Attempts were made to grow the lithium metasilicate from the melt by both Bridgman and Czochralski techniques, with the latter appearing most promising. Milky, polycrystalline boules were all that could be obtained from the Bridgman directional solidification experiments, even when slow growth rates of 0.8 mm/hr were used. The temperature gradient at the melt-crystal interface was about 25 C°/inch in these experiments.

Czochralski crystal pulling experiments on Li_2SiO_3 were performed with two different pieces of equipment. The first ones were with an Arthur D. Little model MP puller heated by an rf induction generator. Since cracking of the boules persisted even after using various shielding and insulation schemes, we decided to use an NRC puller equipped with a very stable resistance furnace built for this puller. The central furnace tube is wound with Pt-10% Rh, and this is surrounded by a larger tube wound with Kanthal. The furnace is equipped with a proportional controller and a Data-Trak for programmable heating and cooling cycles. A special "cover" for shielding above the crucible was fabricated from an inverted kyanite crucible fitted with a side arm and window for viewing. The temperature gradients for the first three inches above the melt varied with shielding designs from 70°/inch to 200°/inch. This cover, the stability of the furnace (less than $\pm 1/2^\circ$ fluctuations), and slow pulling rates of about 2 mm/hr greatly increased the perfection of the boules, but they remained polycrystalline. Nucleating a crystal on the platinum extension to the pulling rod and the necking of crystals has been a problem because of (i) viewing difficulties, (ii) the good shielding and resultant reduced temperature gradients above the melt surface, and (iii) the extreme sensitivity of the crystal diameter

to the furnace temperature. These problems should be eliminated with the use of seeds cut from the polycrystalline boules obtained, and a newly designed viewing port.

The possibility of a phase transition causing the cracking in Li_2SiO_3 was examined by DTA and high temperature x-ray experiments. The DTA experiments showed a small endothermic peak at about 1030° and then the melting point at 1200°C . High temperature x-ray diffraction patterns taken at 835° , 1060° , and 1156° showed only the expected thermal expansion of the orthorhombic unit cell; no new peaks were observed. These high temperature patterns are now being examined to determine if anisotropy in thermal expansion could be great enough to contribute significantly to the cracking problem.

2.2 Fresnoite, $\text{Ba}_2\text{Si}_2\text{TiO}_8$

In previous growth experiments on $\text{Ba}_2\text{Si}_2\text{TiO}_8$, its high melting temperature of 1360°C was difficult to maintain in the center of the insulated platinum crucible without melting the crucible. This problem was overcome by various heat shielding arrangements around the crucible as well as reflectors and shields above the crucible, but only poor quality, cracked crystal boules were obtained. To circumvent the problem in another way, flux-pulling experiments were attempted since the temperature requirements are not so severe. Very small crystals of fresnoite have been grown by slow cooling of TiO_2 -rich melts at the National Bureau of Standards, and our own DTA experiments indicated that additions of TiO_2 to stoichiometric fresnoite lowers the melting temperature significantly. Therefore, we carried out growth experiments after adding various amounts of TiO_2 ranging from 5 to 30 wt.% to fresnoite. In all instances $\text{Ba}_2\text{Si}_2\text{TiO}_8$ could be pulled from these molten solutions, but all the crystal boules contained numerous cracks and appeared more and more milky with increasing amounts of TiO_2 in the melt. With 30 wt.% excess TiO_2 the melting point was lowered about 150°

so that a boule could be grown without extraneous heat shields, but the boules were still cracked. A thin slab of crystal observed under the polarizing microscope showed appreciable amounts of TiO_2 flux intergrown with the fresnoite. Even with slow pulling rates of about 2 mm/hr, the TiO_2 flux inclusions are still a serious problem.

2.3 Lead Potassium Niobate, $\text{Pb}_2\text{KNb}_5\text{O}_{15}$

Several final Czochralski growth experiments were carried out on $\text{Pb}_2\text{KNb}_5\text{O}_{15}$. By varying the content of lead oxide in the melt, small boules of approximately 10 to 15 mm in diameter were grown in which the cracking was reduced. Several oriented and parallel-piped-shaped specimens were prepared for the ultrasonic measurements. When viewed under a polarization microscope one specimen appears to be homogeneous and free of internal strains and is therefore likely to consist of a single domain.

3. X-Ray Determination of Piezoelectric Constants

3.1 Introduction

For the calculation of the electromechanical coupling factor the complete set of piezoelectric constants has to be known. In the present investigation the piezoelectric constants are being determined by measuring by means of x-rays the elastic strain which is induced in a crystal by an applied electric field. This method was first used by Bhalla, Bose, White and Cross (1971) to measure the piezoelectric constant d_{11} of α -quartz. These authors found good agreement with earlier data obtained with other methods. As pointed out by Bhalla, Bose, White and Cross (1971), the x-ray method has several advantages over other methods. Among these are its ready applicability to small crystals (about 1 mm x 1 mm x 0.1 mm) and the possibility to distinguish spontaneous and induced strains in ferroelectric

crystals and to determine the piezoelectric constants of individual domains. In addition, the x-ray method avoids some of the potential difficulties associated with other methods, such as the occurrence of mode coupling in the widely used resonance-antiresonance method (see, e.g., Mason, 1950).

The theoretical equations for the x-ray determination of the complete set of the piezoelectric constants for crystals of all twenty crystal classes which exhibit the piezoelectric effect have been derived. In the following the derivation and the results will be presented, and a numerical example will be discussed.

3.2 Theoretical Derivation

Bragg's form of the condition for constructive reflection of an incident x-ray beam by a lattice plane with Miller indices hkl and interplanar spacing d_{hkl} is given by

$$\sin \theta = \frac{n\lambda}{2d_{hkl}} \quad (1)$$

where

$$\frac{1}{d_{hkl}} = G_{hkl} = (\vec{G}_{hkl} \cdot \vec{G}_{hkl})^{1/2} \quad (2)$$

and

$$\vec{G}_{hkl} = h\vec{a}^* + k\vec{b}^* + l\vec{c}^* \quad (3)$$

denotes a reciprocal lattice vector. \vec{a}^* , \vec{b}^* , \vec{c}^* are the base vectors of the reciprocal lattice defined by $\vec{a} \cdot \vec{a}^* = 1$, $\vec{a} \cdot \vec{b}^* = 0$, etc., where \vec{a} , \vec{b} , \vec{c} are the unit cell vectors of the direct space lattice. If, as in equation (1), the order of the reflection appears explicitly the Miller indices must be assumed to consist of coprime integers (i.e. of integers without a common factor except unity).

By applying an electric field \vec{E} with components $E_r = E\alpha_r$ (α_r are the direction cosines, and $r = 1, 2, 3$ denotes three cartesian coordinate axes) to a crystal, an elastic strain ϵ_{ij} ($i, j = 1, 2, 3$) is induced through the converse piezoelectric effect according to (Nye, 1957)

$$\epsilon_{ij} = d_{rij} E_r, \quad (4)$$

d_{rij} denotes the third rank tensor of the piezoelectric strain constants, and the summation convention is used here and subsequently (i.e. summation over the three values 1, 2, 3 is implied for every pair of identical indices). Of course, the components E_r of the electric field \vec{E} and of the strain tensor ϵ_{ij} , and the set of piezoelectric constants d_{rij} must be referred to a common cartesian coordinate system with axes, x_1, x_2, x_3 .

In order to obtain the dependence of the reciprocal interplanar distance d_{hkl}^{-1} on strain ϵ_{ij} , consider the matrices $\underline{\underline{A}}$ and $\underline{\underline{A}}^*$ composed of the unit cell vectors of the direct and reciprocal lattices, respectively, according to

$$\underline{\underline{A}} = \begin{pmatrix} a_1 & b_1 & c_1 \\ a_2 & b_2 & c_2 \\ a_3 & b_3 & c_3 \end{pmatrix}, \quad \underline{\underline{A}}^* = \begin{pmatrix} a_1^* & b_1^* & c_1^* \\ a_2^* & b_2^* & c_2^* \\ a_3^* & b_3^* & c_3^* \end{pmatrix} \quad (5)$$

The relations $\vec{a} \cdot \vec{a}^* = 1$, $\vec{a} \cdot \vec{b}^* = 0$ etc. can then be written in matrix notation as

$$\underset{\sim}{A} \underset{\sim}{A}^{\star T} = \underset{\sim}{A}^T \underset{\sim}{A}^{\star} = \underset{\sim}{1} \quad (6)$$

where the superscript T denotes the transpose matrix, and $\underset{\sim}{1}$ the unit matrix.

In the approximation of the linear theory of elasticity under the influence of a strain $\underset{\sim}{\varepsilon}$ the base vectors change according to $\underset{\sim}{a}(\varepsilon) = (\underset{\sim}{1} + \underset{\sim}{\varepsilon})\underset{\sim}{a}(0)$, etc., where $\underset{\sim}{\varepsilon}$ denotes the strain tensor ε_{ij} in matrix notation. Therefore, the direct and reciprocal base vector matrices change according to

$$\underset{\sim}{A}(\varepsilon) = (\underset{\sim}{1} + \underset{\sim}{\varepsilon})\underset{\sim}{A}(0) \quad (7a)$$

$$\underset{\sim}{A}^{\star}(\varepsilon) = (\underset{\sim}{1} + \underset{\sim}{\varepsilon})^{-1} \underset{\sim}{A}^{\star}(0) \approx (\underset{\sim}{1} - \underset{\sim}{\varepsilon})\underset{\sim}{A}^{\star}(0) \quad (7b)$$

In the spirit of the linear theory of elasticity, higher than first powers of $\underset{\sim}{\varepsilon}$ have been neglected in the last step of equ. (7b).

According to (7b) a reciprocal lattice vector $\underset{\sim}{G}_{hkl}^{\star}$ changes according to

$$\underset{\sim}{G}_{hkl}^{\star}(\varepsilon) = (\underset{\sim}{1} - \underset{\sim}{\varepsilon})\underset{\sim}{G}_{hkl}^{\star}(0) \quad (8)$$

Therefore,

$$\underset{\sim}{G}_{hkl}^{\star}(\varepsilon) \cdot \underset{\sim}{G}_{hkl}^{\star}(\varepsilon) = \underset{\sim}{G}_{hkl}^{\star}(0) \cdot \underset{\sim}{G}_{hkl}^{\star}(0) - 2(\underset{\sim}{G}_{hkl}^{\star}(0) \cdot \underset{\sim}{\varepsilon} \underset{\sim}{G}_{hkl}^{\star}(0)) \quad (9)$$

and

$$G_{hkl}(\varepsilon) = G_{hkl}(0)(1 - (\vec{N} \cdot \underset{\sim}{\varepsilon} \vec{N})) \quad (10)$$

where

$$\vec{N} = \frac{\vec{G}_{hkl}}{G_{hkl}} \quad (11)$$

denotes the normal of the lattice plane (hkl).

In view of equs. (1), (2), (4) and (10) the diffraction angle θ depends on the magnitude E of the electric field, $\theta = \theta(\vec{\epsilon}(E))$, so that one obtains by differentiation (summation convention!)

$$\left(\frac{\partial \ln \sin \theta}{\partial E} \right) = \left(\frac{\partial \ln G_{hkl}}{\partial \epsilon_{ij}} \right) \left(\frac{\partial \epsilon_{ij}}{\partial E_r} \right) \left(\frac{\partial E_r}{\partial E} \right),$$

or

$$\cot \theta \left(\frac{\partial \theta}{\partial E} \right) = - \alpha_r N_i N_j d_{rij} \quad (12)$$

This relation is the generalized form of equ. (6) of the paper by Bhalla, Bose, White and Cross (1971). For the special case that both the direction of the electric field and the reflecting lattice plane normal are in the x_1 direction, $\alpha_r = \delta_{1r}$, $N_i = \delta_{1i}$, $N_j = \delta_{1j}$ (δ_{mn} denotes the Kronecker symbol, i.e. $\delta_{mn} = 1$ for $m = n = 1, 2, 3$, and $\delta_{mn} = 0$ for $m \neq n$), the above equ. (12) becomes equivalent to equ. (6) of these authors.

Equ. (12) provides the theoretical basis for the experimental determination of the complete set of piezoelectric constants of any piezoelectric material. In order to determine the complete set of piezoelectric constants the dependence of the reflection angle θ on the magnitude of the electric field must be measured for a set of combinations of directions $\vec{\alpha}, \vec{N}$ equal in number to, or if redundancy checks are desired, larger than the number of independent piezoelectric constants corresponding to the crystal class of the material under investigation.

In order to eliminate electrostriction the measurements should be carried out with field reversal which changes the sign of equ. (12), but not of the quadratic electrostriction effect.

Application of the electric field requires a set of thin platelets of the piezoelectric materials with plane parallel electroded faces, so that the direction of one of the two face normals of opposite directions coincides with the direction of $\vec{\alpha} = (\alpha_1 \alpha_2 \alpha_3)$ of the electric field. In practice, the direction of the reflecting lattice planes is restricted to the two cases $\vec{N} \parallel \vec{\alpha}$ and $\vec{N} \perp \vec{\alpha}$. While the former case, corresponding to the reflecting lattice planes parallel to the platelet faces, utilizes the longitudinal piezoelectric effect and is more convenient experimentally, it will be shown that, with the exception of four crystal classes ($\bar{6}$, $\bar{6}m2$, 23 , $\bar{4}3m$) the complete set of piezoelectric constants cannot be determined in this manner. On the other hand, the second configuration, which utilizes the transverse piezoelectric effect and corresponds to the electric field lying in the reflecting planes, requires larger experimental effort to eliminate distortion of the electric field near the side faces of the sample, but permits to determine the complete set of piezoelectric constants for all twenty piezoelectric crystal classes.

In the following section explicit expressions of the right-hand-side of equ. (12) will be given for all twenty piezoelectric crystal classes and for both experimental configurations.

3.3 Application to Piezoelectric Crystal Classes

Denoting for convenience the RHS of equ. (12) by L and T for parallel field and perpendicular-field reflection, corresponding to the longitudinal and transverse piezoelectric effects, respectively, equ. (12) may be rewritten as

$$- \cot \theta \left(\frac{\partial \theta}{\partial E} \right) = \begin{cases} L & (\vec{\alpha} \parallel \vec{N}) \\ T & (\vec{\alpha} \perp \vec{N}) \end{cases} \quad (13)$$

where

$$L = N_i N_j d_{rij} \quad (\vec{\alpha} = \vec{N}) \quad (14a)$$

$$T = \alpha_i N_j d_{rij} \quad (\vec{\alpha} \cdot \vec{N} = 0) \quad (14b)$$

For the numerical application of these equations the form of the piezoelectric constant tensor corresponding to a particular crystal class must be used, and both the lattice plane normal \vec{N} and the direction $\vec{\alpha}$ of the electric field must be expressed in terms of the Miller indices. For the components of the unit vector \vec{N} the corresponding relation is obtained from eqs. (3) and (11) and is for the general triclinic case given by the familiar expression (International Tables for X-Ray Crystallography [1959]) ($i = 1, 2, 3$):

$$N_i = \frac{h a_i^* + k b_i^* + l c_i^*}{[h^2 a^{*2} + k^2 b^{*2} + l^2 c^{*2} + 2klb^*c^* \cos \alpha^* + 2hla^*c^* \cos \beta^* + 2hka^*b^* \cos \gamma^*]^{1/2}} \quad (15)$$

Here a^*, b^*, c^* denotes the lattice constants, and $\alpha^*, \beta^*, \gamma^*$ the angles between the unit cell vectors $\vec{a}^*, \vec{b}^*, \vec{c}^*$ of the reciprocal lattice. a_i^*, b_i^*, c_i^* ($i=1,2,3$) denotes the cartesian coordinates of $\vec{a}^*, \vec{b}^*, \vec{c}^*$, respectively, in the same coordinate system to which the piezoelectric constant tensor is referred.

For parallel field reflection the unit vector $\vec{\alpha}$ is determined by the condition $\vec{\alpha} = \vec{N}$. For perpendicular field reflection $\vec{\alpha}$ is constrained by the condition $\vec{\alpha} \cdot \vec{N} = 0$. Thus for a given lattice plane (hkl) the vector $\vec{\alpha}$ has one degree of freedom, which may be conveniently described by the angle ϕ according to

$$\vec{\alpha} = \cos \phi \vec{U} + \sin \phi \vec{V} \quad (16)$$

where \vec{U} is a unit vector perpendicular to N lying in the plane generated by the unit vector \vec{e}_3 in the x_3 direction, and by the lattice plane normal \vec{N} , and \vec{V} is perpendicular to both \vec{U} and \vec{N} . The vectors \vec{U} and \vec{V} are then given by

$$\vec{U} = (-\vec{e}_3 \cdot \vec{N} \vec{N} + \vec{e}_3) / (N_1^2 + N_2^2)^{1/2} \quad (17a)$$

$$\vec{V} = \vec{U} \times \vec{N} \quad (17b)$$

Inserting (17a) and (17b) into (16), the components α_r of the unit vector $\vec{\alpha}$ may be expressed in terms of the components N_r of the lattice plane normal and of the angle ϕ according to

$$\alpha_1 = - (N_1 N_3 \cos \phi + N_2 \sin \phi) / (N_1^2 + N_2^2)^{1/2} \quad (18a)$$

$$\alpha_2 = - (N_2 N_3 \cos \phi - N_1 \sin \phi) / (N_1^2 + N_2^2)^{1/2} \quad (18b)$$

$$\alpha_3 = (N_1^2 + N_2^2)^{1/2} \cos \phi \quad (18c)$$

As will be discussed below, for most crystal classes convenient choices of the angle ϕ are possible if at least one of the Miller indices is zero. In these cases the vector $\vec{\alpha}$ lies along symmetry directions of the crystal, and a considerable simplification of the equations given below results.

By using the form of the piezoelectric tensor corresponding to the individual crystal classes as given, for example, by Nye (1957) the expressions L and T defined in (14a) and (14b) may be explicitly written out as given below for the twenty piezoelectric crystal classes. In the following, the piezoelectric constants will be expressed in Voigt notation, that is, the index pair ij and d_{rij} (with $r, i, j = 1, 2, 3$) is replaced by a single index $\mu = 1, 2, 3; 4; 5; 6$ corresponding to $ij = 11, 22, 33; 23$ and $32; 13$ and $31; 12$ and 21 , respectively, and a factor of two is introduced for $\mu = 4, 5, 6$, such that

$d_{r\mu} = d_{rij}$ for $\mu = 1, 2, 3$, and $d_{r\mu} = 2d_{rij}$ for $\mu = 4, 5, 6$. The following abbreviations are introduced in order to describe the coefficients of the piezoelectric constants occurring in the expression for T for the tetragonal, trigonal, hexagonal and cubic systems:

$$A_+ = [-2N_1N_2N_3 \cos \phi + (N_1^2 - N_2^2) \sin \phi] N_3 / (N_1^2 + N_2^2)^{1/2} \quad (19a)$$

$$A_- = -N_3 (N_1^2 + N_2^2)^{1/2} \sin \phi \quad (19b)$$

$$B_+ = -N_3^2 (N_1^2 + N_2^2)^{1/2} \cos \phi \quad (19c)$$

$$B_- = -[(N_1^2 - N_2^2) N_3 \cos \phi + 2N_1N_2 \sin \phi] N_3 / (N_1^2 + N_2^2)^{1/2} \quad (19d)$$

$$C_+ = (N_1^2 + N_2^2)^{3/2} \cos \phi \quad (19e)$$

$$C_- = (N_1^2 - N_2^2) (N_1^2 + N_2^2)^{1/2} \cos \phi \quad (19f)$$

$$D_1 = -[(N_1^2 - 3N_2^2) N_1 N_3 \cos \phi + (3N_1^2 - N_2^2) N_2 \sin \phi] / (N_1^2 + N_2^2)^{1/2} \quad (19g)$$

$$D_2 = [(3N_1^2 - N_2^2) N_2 N_3 \cos \phi - (N_1^2 - 3N_2^2) N_1 \sin \phi] / (N_1^2 + N_2^2)^{1/2} \quad (19h)$$

$$E = [(3(N_1^2 + N_2^2) - 2) N_1 N_2 \cos \phi + (N_1^2 - N_2^2) N_3 \sin \phi] / (N_1^2 + N_2^2)^{1/2} \quad (19i)$$

$$F = N_3^2 (N_1^2 + N_2^2)^{1/2} \cos \phi \quad (19j)$$

$$G = N_1 N_2 (N_1^2 + N_2^2)^{1/2} \cos \phi \quad (19k)$$

The description of the direction $\vec{\alpha}$ of the electric field in terms of the angle ϕ as given in equs. (18), and the use of the ϕ -dependent quantities defined in equs. (19a) to (19k) are limited to the case $\vec{N} \neq \vec{e}_3$. For $\vec{N} = \vec{e}_3$ the angle ϕ is not defined. However, the special case $\vec{N}_3 = \vec{e}_3$ is of interest only for the triclinic and monoclinic systems, and the quantity T defined in equ. (14b) becomes in this case

$$T = \alpha_1 d_{13} + \alpha_2 d_{23} \quad (20)$$

On the other hand, for the tetragonal, trigonal, hexagonal and cubic systems the quantity T is identically zero for $\vec{N} = \vec{e}_3$, so that this case need not be considered explicitly.

1. Triclinic System

Class 1(C_1)

(18 independent constants: $d_{11}, d_{12}, d_{13}, d_{14}, d_{15}, d_{16}, d_{21}, d_{22}, d_{23}, d_{24}, d_{25}, d_{26}, d_{31}, d_{32}, d_{33}, d_{34}, d_{35}, d_{36}$)

$$\begin{aligned} L = & N_1^3 d_{11} + N_1 N_2^2 (d_{12} + d_{26}) + N_1 N_3^2 (d_{13} + d_{35}) \\ & + N_1^2 N_2 (d_{21} + d_{16}) + N_2^3 d_{22} + N_2 N_3^2 (d_{23} + d_{34}) \\ & + N_1^2 N_3 (d_{31} + d_{15}) + N_2^2 N_3 (d_{32} + d_{24}) + N_3^3 d_{33} \\ & + N_1 N_2 N_3 (d_{14} + d_{25} + d_{36}) \end{aligned} \quad (21a)$$

$$\begin{aligned} T = & \alpha_1 N_1^2 d_{11} + \alpha_1 N_2^2 d_{12} + \alpha_1 N_3^2 d_{13} \\ & + \alpha_2 N_1^2 d_{21} + \alpha_2 N_2^2 d_{22} + \alpha_2 N_3^2 d_{23} \\ & + \alpha_3 N_1^2 d_{31} + \alpha_3 N_2^2 d_{32} + \alpha_3 N_3^2 d_{33} \\ & + \alpha_1 N_2 N_3 d_{14} + \alpha_1 N_1 N_3 d_{15} + \alpha_1 N_1 N_2 d_{16} \\ & + \alpha_2 N_2 N_3 d_{24} + \alpha_2 N_1 N_3 d_{25} + \alpha_2 N_1 N_2 d_{26} \\ & + \alpha_3 N_2 N_3 d_{34} + \alpha_3 N_1 N_3 d_{35} + \alpha_3 N_1 N_2 d_{36} \end{aligned} \quad (21b)$$

2. Monoclinic System

Class 2(C_2)

(8 independent constants: $d_{14}, d_{16}, d_{21}, d_{22}, d_{23}, d_{25}, d_{34}, d_{36}$)

$$\begin{aligned} L = & N_2^3 d_{22} + N_1^2 N_2 (d_{21} + d_{16}) + N_2 N_3^2 (d_{23} + d_{34}) \\ & + N_1 N_3 N_3 (d_{14} + d_{25} + d_{36}) \end{aligned} \quad (22a)$$

$$\begin{aligned}
 T = & \alpha_2 N_1^2 d_{21} + \alpha_2 N_2^2 d_{22} + \alpha_2 N_3^2 d_{23} \\
 & + \alpha_1 N_2 N_3 d_{14} + \alpha_1 N_1 N_2 d_{16} + \alpha_2 N_1 N_3 d_{25} \\
 & + \alpha_3 N_2 N_3 d_{34} + \alpha_3 N_1 N_2 d_{36}
 \end{aligned} \tag{22b}$$

Class $m(C_9)$

(10 independent constants: $d_{11}, d_{12}, d_{13}, d_{15}, d_{24}, d_{26}, d_{31}, d_{32}, d_{33}, d_{35}$)

$$\begin{aligned}
 L = & N_1^3 d_{11} + N_1 N_2^2 (d_{12} + d_{26}) + N_1 N_3^2 (d_{13} + d_{35}) \\
 & + N_1^2 N_3 (d_{31} + d_{15}) + N_2^2 N_3 (d_{32} + d_{24}) + N_3^3 d_{33}
 \end{aligned} \tag{23a}$$

$$\begin{aligned}
 T = & \alpha_1 N_1^2 d_{11} + \alpha_1 N_2^2 d_{12} + \alpha_1 N_3^2 d_{13} \\
 & + \alpha_3 N_1^2 d_{31} + \alpha_3 N_2^2 d_{32} + \alpha_3 N_3^2 d_{33} \\
 & + \alpha_1 N_1 N_3 d_{15} + \alpha_2 N_2 N_3 d_{24} + \alpha_2 N_1 N_2 d_{26} + \alpha_3 N_1 N_3 d_{35}
 \end{aligned} \tag{23b}$$

3. Orthorhombic System

Class $222(D_2)$

(3 independent constants: d_{14}, d_{25}, d_{36})

$$L = N_1 N_2 N_3 (d_{14} + d_{25} + d_{36}) \tag{24a}$$

$$T = \alpha_1 N_2 N_3 d_{14} + \alpha_2 N_1 N_3 d_{25} + \alpha_3 N_1 N_2 d_{36} \tag{24b}$$

Class $mm2(C_{2v})$

(5 independent constants: $d_{15}, d_{24}, d_{31}, d_{32}, d_{33}$)

$$L = N_1^2 N_3 (d_{31} + d_{15}) + N_2^2 N_3 (d_{32} + d_{24}) + N_3^2 d_{33} \tag{25a}$$

$$\begin{aligned}
 T = & \alpha_3 N_1^2 d_{31} + \alpha_3 N_2^2 d_{32} + \alpha_3 N_3^2 d_{33} \\
 & + \alpha_1 N_1 N_3 d_{15} + \alpha_2 N_2 N_3 d_{24}
 \end{aligned} \tag{25b}$$

4. Tetragonal System

Class 4(C₄)

(4 independent constants: d_{14} , d_{15} , d_{31} , d_{33})

$$L = (N_1^2 + N_2^2)N_3(d_{31} + d_{15}) + N_3^3d_{33} \quad (26a)$$

$$T = C_+d_{31} + Fd_{33} + A_-d_{14} + B_+d_{15} \quad (26b)$$

Class $\bar{4}$ (S₄)

(4 independent constants: d_{14} , d_{15} , d_{31} , d_{36})

$$L = (N_1^2 - N_2^2)N_3(d_{31} + d_{15}) + N_1N_2N_3(2d_{14} + d_{36}) \quad (27a)$$

$$T = C_-d_{31} + A_+d_{14} + B_-d_{15} + Gd_{36} \quad (27b)$$

Class 422(D₄)

(1 independent constant: d_{14})

$$L = 0 \quad (28a)$$

$$T = A_-d_{14} \quad (28b)$$

Class 4mm(C_{4v})

(3 independent constants: d_{15} , d_{31} , d_{33})

$$L = (N_1^2 + N_2^2)N_3(d_{31} + d_{15}) + N_3^3d_{33} \quad (29a)$$

$$T = C_+d_{31} + Fd_{33} + B_+d_{15} \quad (29b)$$

Class $\bar{4}2m$ (D_{2d})

(2 independent constants: d_{14} , d_{36})

$$L = N_1N_2N_3(2d_{14} + d_{36}) \quad (30a)$$

$$T = A_+d_{14} + Gd_{36} \quad (30b)$$

5. Trigonal System

Class 3(C₃)

(6 independent constants: $d_{11}, d_{14}, d_{15}, d_{22}, d_{31}, d_{33}$)

$$L = (N_1^2 - 3N_2^2)N_1d_{11} - (3N_1^2 - N_2^2)N_2d_{22} + N_3^3d_{33} \\ + (N_1^2 + N_2^2)N_3(d_{31} + d_{15}) \quad (31a)$$

$$T = D_1d_{11} + D_2d_{22} + C_+d_{31} + Fd_{33} + A_-d_{14} + B_+d_{15} \quad (31b)$$

Class 32(D₃)

(2 independent constants: d_{11}, d_{14})

$$L = (N_1^2 - 3N_2^2)N_1d_{11} \quad (32a)$$

$$T = D_1d_{11} + A_-d_{14} \quad (32b)$$

Class 3m(C_{3v})

(4 independent constants: $d_{15}, d_{22}, d_{31}, d_{33}$)

$$L = - (3N_1^2 - N_2^2)N_2d_{ss} + (N_1^2 + N_2^2)N_3(d_{31} + d_{15}) + N_3^3d_{33} \quad (33a)$$

$$T = D_2d_{22} + C_+d_{31} + Fd_{33} + B_+d_{15} \quad (33b)$$

6. Hexagonal System

Class 6(C₆)

(4 independent constants: $d_{14}, d_{15}, d_{31}, d_{33}$)

$$L = (N_1^2 + N_2^2)N_3(d_{31} + d_{15}) + N_3^3d_{33} \quad (34a)$$

$$T = C_+d_{31} + Fd_{33} + A_-d_{14} + B_+d_{15} \quad (34b)$$

Class 6(C_{3h})

(2 independent constants: d_{11}, d_{22})

$$L = (N_1^2 - 3N_2^2)N_1d_{11} - (3N_1^2 - N_2^2)N_2d_{22} \quad (35a)$$

$$T = D_1d_{11} + D_2d_{22} \quad (35b)$$

Class 622(D₆)

(1 independent constant: d_{14})

$$L = 0 \quad (36a)$$

$$T = A_- d_{14} \quad (36b)$$

Class 6mm(C_{6v})

(3 independent constants: d_{15} , d_{31} , d_{33})

$$L = (N_1^2 + N_2^2)N_3(d_{31} + d_{15}) + N_3^3 d_{33} \quad (37a)$$

$$T = C_+ d_{31} + F d_{33} + B_+ d_{15} \quad (37b)$$

Class $\bar{6}m2(D_{3h})$

(1 independent constant: d_{11})

$$L = (N_1^2 - 3N_2^2)N_1 d_{11} \quad (38a)$$

$$T = D_1 d_{11} \quad (38b)$$

Classes 23(T) and $\bar{4}3m(T_d)$

(1 independent constant: d_{14})

$$L = 3N_1 N_2 N_3 d_{14} \quad (39a)$$

$$T = E d_{14} \quad (39b)$$

As mentioned above, equations (26b), (27b), etc., to (39b) are valid only for $\vec{N} \neq \vec{e}_3$, and for $\vec{N} = \vec{e}_3$ the quantity T in these equations is identically zero.

Equations (21a) to (39a) represent the most general form of the expressions for the longitudinal piezoelectric effect for the 20 piezoelectric crystal classes. Each lattice plane (hkl) is characterized by its effective piezoelectric coefficient $L = L_{hkl}$, which is for triclinic symmetry obtained by inserting equ. (15) into equ. (21a), and for the crystal classes of higher

symmetry by inserting the simplified form of equ. (15) appropriate for the particular crystal symmetry into the corresponding equs. (22a) to (39a). For each lattice plane (hkl) the electric field coefficient $-\cot \theta$ ($\partial \theta / \partial E$) of the Bragg angle $\theta = \theta_{hkl}$ gives according to equ. (13) an experimental value for the corresponding linear combination L_{hkl} of piezoelectric constants. While no further simplification is possible for triclinic symmetry, it will be shown below that for the crystal classes of higher symmetry the expressions for L given by equs. (22a) to (39a) may become much simpler if one or two of the Miller indices are zero. However, in several instances the coefficients of the piezoelectric constants in the expressions for L vanish, unless all three Miller indices are nonzero. Thus for the experimental determination of the complete set of piezoelectric constants the most general form of the expressions for L as given in equs. (21a) to (39a) has to be used.

Similarly, equations (21b) to (39b) represent the most general form of the expressions for the transverse piezoelectric effect in terms of the components of the reflecting lattice plane normal \vec{N} , the direction $\vec{\alpha}$ of the electric field, and the coefficients A_+ , A_- etc. defined in equs. (19a) to (19k). According to equs. (18a) to (18c) the components of $\vec{\alpha}$, and according to equs. (19a) to (19k) the coefficients A_+ , A_- , etc. depend on the components of \vec{N} and on the free parameter ϕ defined in equ. (16). The components of \vec{N} , in turn, depend on the Miller indices according to equ. (15). Thus all coefficients of the piezoelectric constants in the expressions for T depend on the Miller indices in a rather involved manner. While for triclinic symmetry the equations have to be used in this form, a considerable simplification occurs if one or two of the Miller indices are zero. However, for the two monoclinic crystal classes 2 and m the coefficients of some piezoelectric constants (those of d_{14} and d_{34} for class 2, and of d_{24} for class m) vanish

in these special cases. Therefore the complete set of piezoelectric constants cannot be determined only from measurements of the transverse piezoelectric effect perpendicular to these special lattice planes. In these cases one has to use the general form of equations (22b) and (23b) for the transverse piezoelectric effect or, alternatively, supplement the equations for the transverse piezoelectric effect for the special set of lattice planes with one Miller index zero by the general equations (22a) and (23a) for the longitudinal piezoelectric effect.

In Tables 1 to 5 the simplified relations obtained from equs. (22a) and (22b) to (38a) and (38b) are presented that result for the longitudinal and transverse piezoelectric coefficients L and T in the monoclinic, orthorhombic, tetragonal, trigonal and hexagonal classes if at least one of the Miller indices is zero. For the monoclinic and orthorhombic classes the general expressions for the longitudinal piezoelectric coefficients L have also been included because they are needed for the experimental determination of the complete set of piezoelectric constants. For completeness, the equation for L for the two isometric classes 23 and $\bar{4}3m$ is also presented as Table 6. The explanation of Tables 1 to 6 is given below.

The simpler equations presented in Tables 1 to 6 are sufficient for the experimental determination of the complete set of piezoelectric constants for all crystal classes, except for triclinic symmetry. Therefore the general form of the equations (22a) and (22b) to (39a) and (39b) need not be considered in the design of actual experiments. It may happen in certain cases, however, that for the lattice planes with at least one Miller index zero that are listed in Tables 1 to 6 the structure factor may be inconveniently small, or vanish exactly. In these cases and for triclinic symmetry one has to resort to the general equations (21) to (39).

Table 1. Crystal plate normal $\vec{\alpha} = (\alpha_1, \alpha_2, \alpha_3)$, Miller indices hkl , face normal of reflecting plane $\vec{N} = (N_1, N_2, N_3)$, and expressions for L and T defined in equations (14a) and (14b) for monoclinic system.[†]
The base vectors \vec{b} and \vec{c} coincide with the Y and Z axes, respectively, and the base vector \vec{a} lies in the X - Z plane, forming an angle $\beta > 90^\circ$ with the \vec{c} axis.

Class	$\vec{\alpha}$	(hkl)	\vec{N}	$\xi; \eta; \zeta; R$	L, T
(C_2) 3 constants)	(010)	(0k0)	(010)		$L = d_{22}$
		(h0l)	(ξ0ζ)	$\xi = (ha^* - lc^*)/R; \zeta = lc^*S/R$ $R = [h^2a^{*2} + l^2c^{*2} - 2hla^*c^*C]^{1/2}$	$T = \xi^2 d_{21} + \zeta^2 d_{23} + \xi \zeta d_{25}$
	(001)	(hk0)	(ξη0)	$\xi = ha^*/R; \eta = kb^*/R$ $R = [h^2a^{*2} + k^2b^{*2}]^{1/2}$	$T = \xi \eta d_{36}$
	($\bar{\eta}\xi 0$)	(hk0)	(ξη0)	$\xi = ha^*/R; \eta = kb^*/R$ $R = [h^2a^{*2} + k^2b^{*2}]^{1/2}$	$T = \xi^3 d_{21} + \xi \eta^2 d_{22} - \xi \eta^2 d_{16}$
	(ξηζ)	(hkl)	(ξηζ)	$\xi = (ha^* - lc^*)/R; \eta = kb^*/R; \zeta = lc^*S/R$ $R = [h^2a^{*2} + k^2b^{*2} + l^2c^{*2} - 2hla^*c^*C]^{1/2}$	$L = \eta^3 d_{22} + \xi^2 \eta (d_{21} + d_{16}) + \eta \zeta^2 (d_{23} + d_{34}) + \xi \eta \zeta (d_{14} + d_{25} + d_{36})$
(C_s) 10 constants)	(100)	(h00)	(100)		$L = d_{11}$
		(0k0)	(010)		$T = d_{12}$
	(001)	(hk0)	(ξη0)	$\xi = ha^*/R; \eta = kb^*/R$ $R = [h^2a^{*2} + k^2b^{*2}]^{1/2}$	$T = \xi^2 d_{31} + \eta^2 d_{32}$
	($\bar{\eta}\xi 0$)	(hk0)	(ξη0)	$\xi = ha^*/R; \eta = kb^*/R$ $R = [h^2a^{*2} + k^2b^{*2}]^{1/2}$	$T = -\xi^2 \eta d_{11} - \eta^3 d_{12} + \xi^2 \eta d_{26}$
	($\bar{\zeta} 0 \xi$)	(h0l)	(ξ0ζ)	$\xi = (ha^* - lc^*)/R; \zeta = lc^*S/R$ $R = [h^2a^{*2} + l^2c^{*2} - 2hla^*c^*C]^{1/2}$	$T = -\xi^2 \zeta d_{11} - \zeta^3 d_{13} + \xi^3 d_{31} + \xi \zeta^2 d_{33} - \xi \zeta^2 d_{15} + \xi^2 \zeta d_{35}$
	(ξ0ζ)	(h0l)	(ξ0ζ)	$\xi = (ha^* - lc^*)/R; \zeta = lc^*S/R$ $\zeta = [h^2a^{*2} + l^2c^{*2} - 2hla^*c^*C]^{1/2}$	$L = \xi^3 d_{11} + \xi \zeta^2 (d_{13} + d_{35}) + \xi^2 \zeta (d_{31} + d_{15}) + \zeta^3 d_{33}$
	(ξηζ)	(hkl)	(ξηζ)	$\xi = (ha^* - lc^*)/R; \eta = kb^*/R; \zeta = lc^*S/R$ $R = [h^2a^{*2} + k^2b^{*2} + l^2c^{*2} - 2hla^*c^*C]^{1/2}$	$L = \xi^3 d_{11} + \xi \eta^2 (d_{12} + d_{26}) + \xi \zeta^2 (d_{13} + d_{35}) + \xi^2 \zeta (d_{31} + d_{15}) + \eta^2 \zeta (d_{32} + d_{24}) + \zeta^3 d_{33}$

$$a^* = 1/a \sin \beta; b^* = 1/b; c^* = 1/c \sin \beta; C = \cos \beta; S = \sin \beta$$

Table 2. Crystal plate normal $\vec{\alpha} = (\alpha_1, \alpha_2, \alpha_3)$, Miller indices hkl , face normal of reflecting plane $\vec{N} = (N_1, N_2, N_3)$ and expressions for L and T defined in equations (14a) and (14b) for orthorhombic system.

Class	$\vec{\alpha}$	(hkl)	\vec{N}	$\xi; \eta; \zeta; R$	L, T
222(D_2) (3 constants)	(100)	(0kl)	(0 $\eta\zeta$)	$\eta = k/bR; \zeta = l/cR$ $R = [k/b]^2 + (l/c)^2]^{1/2}$	$T = \eta\zeta d_{14}$
	(010)	(h0l)	($\xi 0\zeta$)	$\xi = h/aR; \zeta = l/cR$ $R = [(h/a)^2 + (l/c)^2]^{1/2}$	$T = \xi\zeta d_{25}$
	(001)	(hk0)	($\xi\eta 0$)	$\xi = h/aR; \eta = k/bR$ $R = [(h/a)^2 + (k/b)^2]^{1/2}$	$T = \xi\eta d_{36}$
	($\xi\eta\zeta$)	(hkl)	($\xi\eta\zeta$)	$\xi = h/aR; \eta = k/bR; \zeta = l/cR$ $R = [(h/a)^2 + (k/b)^2 + (l/c)^2]^{1/2}$	$L = \xi\eta\zeta(d_{14} + d_{25} + d_{36})$
$mm2(C_{2v})$ (5 constants)	(001)	(hk0)	($\xi\eta 0$)	$\xi = h/aR; \eta = k/bR$ $R = [(h/a)^2 + (k/b)^2]^{1/2}$	$T = \xi^2 d_{31} + \eta^2 d_{32}$
		(00l)	(001)		$L = d_{33}$
	($\bar{\zeta} 0 \xi$)	(h0l)	($\xi 0 \zeta$)	$\xi = h/aR; \zeta = l/cR$ $R = [(h/a)^2 + (l/c)^2]^{1/2}$	$T = \xi^3 d_{31} + \xi\zeta^2 d_{33} - \xi\zeta^2 d_{15}$
	(0 $\bar{\zeta}$ η)	(0kl)	(0 $\eta\zeta$)	$\eta = k/bR; \zeta = l/cR$ $R = [(k/b)^2 + (l/c)^2]^{1/2}$	$T = \eta^3 d_{32} + \eta\zeta^2 d_{33} - \eta\zeta^2 d_{24}$
	($\xi\eta\zeta$)	(hkl)	($\xi\eta\zeta$)	$\xi = h/aR; \eta = k/bR; \zeta = l/cR$ $R = [(h/a)^2 + (k/b)^2 + (l/c)^2]^{1/2}$	$L = \xi^2\zeta(d_{31} + d_{15}) + \eta^2\zeta(d_{32} + d_{24}) + \zeta^3 d_{33}$

Table 3. Crystal plate normal $\vec{\alpha} = (\alpha_1, \alpha_2, \alpha_3)$, Miller indices hkl , face normal of reflecting plane $\vec{N} = (N_1, N_2, N_3)$, and expressions for L and T defined in equations (14a) and (14b) for tetragonal system.

Class	$\vec{\alpha}$	(hkl)	\vec{N}	$\xi; \eta; \zeta; R$	L, T
$4(C_4)$ (4 constants)	(100)	(0kl)	(0 $\eta\zeta$)	$\eta = k/aR; \zeta = l/cR$ $R = [(k/a)^2 + (l/c)^2]^{1/2}$	$T = \eta\zeta d_{14}$
	(001)	(00l)	(001)		$L = d_{33}$
		(hk0)	($\xi\eta 0$)	$\xi = h/R; \eta = k/R$ $R = [h^2 + k^2]^{1/2}$	$T = d_{31}$
	($\bar{\zeta}0\xi$)	(h0l)	($\xi 0\zeta$)	$\xi = h/aR; \zeta = l/cR$ $R = [(h/a)^2 + (l/c)^2]^{1/2}$	$T = \xi^3 d_{31} + \xi\zeta^2 d_{33} - \xi\zeta^2 d_{15}$
$\bar{4}(S_4)$ (4 constants)	(100)	(0kl)	(0 $\eta\zeta$)	$\eta = k/aR; \zeta = l/cR$ $R = [(k/a)^2 + (l/c)^2]^{1/2}$	$T = \eta\zeta d_{14}$
	(001)	(hk0)	($\xi\eta 0$)	$\xi = h/R; \eta = k/R$ $R = [h^2 + k^2]^{1/2}$	$T = (\xi^2 - \eta^2) d_{31} + \xi\eta d_{36}$
	($\bar{\zeta}0\xi$)	(h0l)	($\xi 0\zeta$)	$\xi = h/aR; \zeta = l/cR$ $R = [(h/a)^2 + (l/c)^2]^{1/2}$	$T = \xi^3 d_{31} - \xi\zeta^2 d_{15}$
$422(D_4)$ (1 constant)	(100)	(0kl)	(0 $\eta\zeta$)	$\eta = k/aR; \zeta = l/cR$ $R = [(k/a)^2 + (l/c)^2]^{1/2}$	$T = \eta\zeta d_{14}$
$4mm(C_{4v})$ (3 constants)	(001)	(00l)	(001)		$L = d_{33}$
		(hk0)	($\xi\eta 0$)	$\xi = h/R; \eta = k/R$ $R = [h^2 + k^2]^{1/2}$	$T = d_{31}$
	($\bar{\zeta}0\xi$)	(h0l)	($\xi 0\zeta$)	$\xi = h/aR; \zeta = l/cR$ $R = [(h/a)^2 + (l/c)^2]^{1/2}$	$T = \xi^3 d_{31} + \xi\zeta^2 d_{33} - \xi\zeta^2 d_{15}$
$\bar{4}2m(D_{2d})$ (2 constants)	(100)	(0kl)	($\eta\eta\zeta$)	$\eta = k/aR; \zeta = l/cR$ $R = [(k/a)^2 + (l/c)^2]^{1/2}$	$T = \eta\zeta d_{14}$
	(001)	(hk0)	($\xi\eta 0$)	$\xi = h/R; \eta = k/R$ $R = [h^2 + k^2]^{1/2}$	$T = \xi\eta d_{36}$

Table 4. Crystal plate normal $\vec{\alpha} = (\alpha_1, \alpha_2, \alpha_3)$, Miller-Bravais indices hkl , for hexagonal indexing, face normal of reflecting plane $\vec{N} = (N_1, N_2, N_3)$, and expressions L and T defined in equations (14a) and (14b) for trigonal system.

Class	$\vec{\alpha}$	(hkl)	\vec{N}	$\xi; \eta; \zeta; R$	L, T
$3(C_3)$ (6 constants)	(100)	$(2h, \bar{h}, 0)$ $(0kl)$	(100) $(0\eta\zeta)$	$\eta = 2k/\sqrt{3}aR; \zeta = l/cR$ $R = [(4/3)(k/a)^2 + (l/c)^2]^{1/2}$	$L = d_{11}$ $T = -\eta^2 d_{11} + \eta \zeta d_{14}$
	(010)	$(0k0)$ $(2h, \bar{h}, l)$	(010) $(\xi 0 \zeta)$	$\xi = 2h/aR; \zeta = l/cR$ $R = [(2h/a)^2 + (l/c)^2]^{1/2}$	$L = d_{22}$ $T = -\xi^2 d_{22} - \xi \zeta d_{14}$
	(001)	$(00l)$ $(2h, k-h, 0)$	(001) $(\xi \eta 0)$	$\xi = \sqrt{3}h/R; \eta = k/R$ $R = [3h^2 + k^2]^{1/2}$	$L = d_{33}$ $T = d_{31}$
	$(0\eta\zeta)$	$(0kl)$	$(0\eta\zeta)$	$\eta = 2k/\sqrt{3}aR; \zeta = l/cR$ $R = [(4/3)(k/a)^2 + (l/c)^2]^{1/2}$	$L = \eta^3 d_{22} + \zeta^3 d_{33} + \eta^2 \zeta (d_{31} + d_{15})$
	$(0\bar{\zeta}\eta)$	$(0kl)$	$(0\eta\zeta)$	$\eta = 2k/\sqrt{3}aR; \zeta = l/cR$ $R = [(4/3)(k/a)^2 + (l/c)^2]^{1/2}$	$T = -\eta^2 \zeta d_{22} + \eta \zeta^2 d_{33} + \eta^3 d_{31} - \eta \zeta^2 d_{15}$
$32(D_3)$ (2 constants)	(100)	$(2h, \bar{h}, 0)$ $(0kl)$	(100) $(0\eta\zeta)$	$\eta = 2k/\sqrt{3}aR; \zeta = l/cR$ $R = [(4/3)(k/a)^2 + (l/c)^2]^{1/2}$	$L = d_{11}$ $T = -\eta^2 d_{11} + \eta \zeta d_{14}$
$3m(C_{3v})$ (4 constants)	(010)	$(0k0)$	(010)		$L = d_{22}$
	(001)	$(00l)$	(001)		$L = d_{33}$
		$(2h, k-h, 0)$	$(\xi \eta 0)$	$\xi = \sqrt{3}h/R; \eta = k/R$ $R = [3h^2 + k^2]^{1/2}$	$T = d_{31}$
	$(0\eta\zeta)$	$(0kl)$	$(0\eta\zeta)$	$\eta = 2k/\sqrt{3}aR; \zeta = l/cR$ $R = [(4/3)(k/a)^2 + (l/c)^2]^{1/2}$	$L = \eta^3 d_{22} + \zeta^3 d_{33} + \eta^2 \zeta (d_{31} + d_{15})$
	$(0\bar{\zeta}\eta)$	$(0kl)$	$(0\eta\zeta)$	$\eta = 2k/\sqrt{3}aR; \zeta = l/cR$ $R = [(4/3)(k/a)^2 + (l/c)^2]^{1/2}$	$T = -\eta^2 \zeta d_{22} + \eta \zeta^2 d_{33} + \eta^3 d_{31} - \eta \zeta^2 d_{15}$

Table 5. Crystal plate normal $\vec{\alpha} = (\alpha_1, \alpha_2, \alpha_3)$, Miller-Bravais indices hkl , face normal of reflecting plane $\vec{N} = (N_1, N_2, N_3)$, and expressions L and T defined in equations (14a) and (14b) for hexagonal system.

Class	$\vec{\alpha}$	(hkl)	\vec{N}	$\xi; \eta; \zeta; R$	L, T
$6(C_6)$ (4 constants)	(100)	(0k ℓ)	(0 $\eta\zeta$)	$\eta = 2k/\sqrt{3}aR; \zeta = \ell/cR$ $R = [(4/3)(k/a)^2 + (\ell/c)^2]^{1/2}$	$T = \eta\zeta d_{14}$
	(001)	(00 ℓ)	(001)		$L = d_{33}$
		(2h, k-h, 0)	($\xi\eta 0$)	$\xi = \sqrt{3}h/R; \eta = k/R$ $R = [3h^2 + k^2]^{1/2}$	$T = d_{31}$
	(0 $\eta\zeta$)	(0k ℓ)	(0 $\eta\zeta$)	$\eta = 2k/\sqrt{3}aR; \zeta = \ell/cR$ $R = [(4/3)(k/a)^2 + (\ell/c)^2]^{1/2}$	$L = \zeta^3 d_{33} + \eta^2 \zeta (d_{31} + d_{15})$
	(0 $\bar{\zeta}\eta$)	(0k ℓ)	(0 $\eta\zeta$)	$\eta = 2k/\sqrt{3}aR; \zeta = \ell/cR$ $R = [(4/3)(k/a)^2 + (\ell/c)^2]^{1/2}$	$T = \eta\zeta^2 d_{33} + \eta^3 d_{31} - \eta\zeta^2 d_{15}$
$\bar{6}(C_{3h})$ (2 constants)	(100)	(2h, \bar{h} , 0)	(100)		$L = d_{11}$
	(010)	(0k0)	(010)		$L = d_{22}$
$622(D_6)$ (1 constant)	(100)	(0k ℓ)	(0 $\eta\zeta$)	$\eta = 2k/\sqrt{3}aR; \zeta = \ell/cR$ $R = [(4/3)(k/a)^2 + (\ell/c)^2]^{1/2}$	$T = \eta\zeta d_{14}$
$6mm(C_{6v})$ (3 constants)	(001)	(00 ℓ)	(001)		$L = d_{33}$
		(2h, k-h, 0)	($\xi\eta 0$)	$\xi = \sqrt{3}h/R; \eta = k/R$ $R = [3h^2 + k^2]^{1/2}$	$T = d_{31}$
	(0 $\eta\zeta$)	(0k ℓ)	(0 $\eta\zeta$)	$\eta = 2k/\sqrt{3}aR; \zeta = \ell/cR$ $R = [(4/3)(k/a)^2 + (\ell/c)^2]^{1/2}$	$L = \zeta^3 d_{33} + \eta^2 \zeta (d_{31} + d_{15})$
	(0 $\bar{\zeta}\eta$)	(0k ℓ)	(0 $\eta\zeta$)	$\eta = 2k/\sqrt{3}aR; \zeta = \ell/cR$ $R = [(4/3)(k/a)^2 + (\ell/c)^2]^{1/2}$	$T = \eta\zeta^2 d_{33} + \eta^3 d_{31} - \eta\zeta^2 d_{15}$
$\bar{6}m2(D_{3h})$ (1 constant)	(100)	(2h, \bar{h} , 0)	(100)		$L = d_{11}$

Table 6. Crystal plate normal, Miller indices (hkl) , face normal of reflecting plane $\vec{N} = (N_1 N_2 N_3)$, and expression L defined in equation (1/a) for isometric classes 23 and $\bar{4}3m$.

$\vec{\alpha}$	(hkl)	\vec{N}	$\xi; \eta; \zeta; R$	L
$(\xi\eta\zeta)$	(hkl)	$(\xi\eta\zeta)$	$\xi=h/R; \eta=k/R; \zeta=l/R$ $R=[h^2+k^2+l^2]^{1/2}$	$3\xi\eta\zeta d_{14}$

It is apparent from equations (21a), (22a), etc., to (39a), that some of the piezoelectric constants enter the expressions for L only in the form of linear combinations, so that the complete set of piezoelectric constants cannot be determined from parallel-field reflection measurements ($\vec{\alpha} = \vec{N}$) alone. Exceptions are the four classes $\bar{6}$, $\bar{6}m2$, 23, and $\bar{4}3m$, for which the quantity L depends on the individual piezoelectric constants only, so that they can be determined from parallel-field reflection alone. For all other classes, perpendicular-field reflection measurements ($\vec{\alpha}_3 \cdot \vec{N} = 0$) are required in addition to, or instead of parallel-field reflection measurements.

Another noteworthy feature of the above equations is that for the six classes 4, 422, 3, 32, 6, 622, the piezoelectric constant d_{14} does not enter the equations for L and therefore cannot at all be determined from parallel-field reflection measurements.

According to equations (21b), (22b), etc., to (39b) the quantity T depends in all cases on all individual piezoelectric constants. Exceptions are particular directions of \vec{N} and/or values of ϕ , for which some of the coefficients given in equations (19a) to (19k) may become equal, or vanish. In general, however, it is possible to determine the complete set of piezoelectric constants from a sufficiently large number of perpendicular-field reflection measurements alone. In practice, however, it is desirable to use as many parallel-field reflection measurements as possible, because the specimen preparation is simpler and experimental errors may be expected to be smaller in this case.

3.4 Specimen Orientation

For the measurement of the longitudinal piezoelectric effect crystal platelets with electroded pairs of (hkl) faces with normal $\vec{N} = \vec{\alpha}$ are required. For the transverse piezoelectric effect platelets with electroded pairs of faces with normal $\vec{\alpha}$ perpendicular to the normal \vec{N} of the reflecting (hkl) face must be prepared. In both cases it is desirable to choose the direction \vec{N} , and in the second case also the direction $\vec{\alpha}$, along high symmetry directions (parallel to rotation axes, perpendicular to or within mirror planes) so as to achieve accurate orientation and reduce the effort required for the orientation and preparation of the platelets. However, since either or both piezoelectric effects may vanish along some symmetry directions the requirement of non-vanishing piezoelectric effect eliminates many otherwise suitable lattice planes. It is further desirable, that for a given platelet normal $\vec{\alpha}$ several non-equivalent side faces (hkl) exist, which lead to different linear combinations of piezoelectric constants in the expression for the transverse piezoelectric coefficient T . Ideally, it would be desirable to determine the complete set of piezoelectric constants from one polygon-shaped crystal platelet with several side-faces, so as to require only one pair of electroded surfaces for measuring the longitudinal piezoelectric effect in the direction of the plate normal $\vec{\alpha}$, and the transverse effect for several non-equivalent side face normals \vec{N} . Unfortunately, this ideal design is possible only for some of the high symmetry crystal classes. In general, more than one type of crystal platelet is required for determining the complete set of piezoelectric constants. In this case it is desirable to perform the measurements mostly, or if possible, exclusively on the basis of the longitudinal effect, because the corresponding platelets require only one pair of parallel faces and are

therefore easier to prepare than platelets for the measurement of the transverse effect, and because measurements of the longitudinal effect can be done more accurately and more easily than those of the transverse effect. As mentioned above, this can only be achieved for the four classes $\bar{6}$, $\bar{6}m2$, 23 and $\bar{4}3m$.

For the triclinic system no symmetry directions exist, so that (at least) 18 platelets corresponding to 18 different face normals $\vec{\alpha}$ are required. Since according to equation (21a) the longitudinal piezoelectric coefficient L depends on 10 linear combinations of piezoelectric constants, 10 of the 18 platelets may be chosen such that their faces correspond to 10 different (hkl) planes. The remaining (minimum of) 8 platelets must be prepared for the transverse piezoelectric effect in such a manner that the normals $\vec{\alpha}$ of the pair of large electroded surfaces are perpendicular to 8 different (hkl) side faces. The resulting piezoelectric coefficients depend on the orientation of the crystallographic axes with respect to the cartesian coordinate system chosen. It is recommended to use the base vectors of the direct and reciprocal lattice according to the 1949 IRE convention (Standards on Piezoelectric Crystals, 1949):

$$\vec{a} = (a \sin \beta, \quad 0, \quad a \cos \beta)$$

$$\vec{b} = (-b \sin \alpha \cos \gamma^*, \quad b \sin \alpha \sin \gamma^*, \quad b \cos \alpha)$$

$$\vec{c} = (0, \quad 0, \quad c)$$

$$\vec{a}^* = (a^* \sin \gamma^*, \quad a^* \cos \gamma^*, \quad 0)$$

$$\vec{b}^* = (0, \quad b^*, \quad 0)$$

$$\vec{c}^* = (-c^* \sin \alpha^* \cos \beta, \quad c^* \cos \alpha^*, \quad c^* \sin \alpha^* \sin \beta)$$

Here it is (International Tables for X-Ray Crystallography, 1959):

$$a^* = \frac{bc \sin \alpha}{V}, \text{ etc.},$$

$$V = 2abc \sin \frac{\alpha+\beta+\gamma}{2} \sin \frac{-\alpha+\beta+\gamma}{2} \sin \frac{\alpha-\beta+\gamma}{2} \sin \frac{\alpha+\beta-\gamma}{2}$$

$$\cos \alpha^* = (\cos \beta \cos \gamma - \cos \alpha) / \sin \beta \sin \gamma, \text{ etc.}$$

It is further $\alpha > 90^\circ$, $\beta > 90^\circ$.

For the symmetry classes of higher symmetry the 1949 IRE convention (Standards on Piezoelectric Crystals, 1949) is easily summarized as follows. The twofold axes of class $2(C_2)$, and the mirror plane normal of class $m(C_s)$ coincide with the crystallographic \vec{b} axis, which is placed along the positive Y direction of a right-handed cartesian coordinate system. The \vec{c} -axis is placed along the positive Z-direction, and the \vec{a} -axis (being normal to the \vec{b} -axis and forming an angle $\beta > 90^\circ$ with the \vec{c} -axis) is lying in the XZ-plane. For the orthorhombic, tetragonal and cubic systems the crystallographic axes coincide with the X, Y and Z-axes. For the trigonal and hexagonal systems the threefold (or sixfold) axis is parallel to the Z-axis, and the positive X-axis coincides with any of the three secondary axes $\vec{a}_1, \vec{a}_2, \vec{a}_3$ perpendicular to the threefold (or sixfold) axes. The Y-axis is perpendicular to the X- and Z-axes, so as to form a right-handed cartesian coordinate system.

3.5 Discussion of Tables 1 to 6

For the remaining 19 piezoelectric crystal classes the existence of symmetry elements reduces not only the number of independent piezoelectric constants, but also leads to the existence of high-symmetry directions $\vec{\alpha}$ with non-vanishing longitudinal and/or transverse piezoelectric effect. In Table 1 to 6 such pairs of high-symmetry directions $\vec{\alpha}, \vec{N}$, the associated Miller indices hkl and the quantities L or T describing the

longitudinal and transverse piezoelectric effect as defined in equations (14a) and (14b) are listed for the crystal classes of the monoclinic, orthorhombic, tetragonal, trigonal, hexagonal and cubic systems, respectively. In the crystal classes of lower symmetry the number of high symmetry directions is too small for determining the complete set of the piezoelectric constants. In these cases the expressions for both $\vec{\alpha}$ and \vec{N} and for the associated values of L and/or T are also given for a general set of Miller indices.

The results in Table 1 indicate that for the class $C_2(2)$ the 8 independent constants may be determined from 5 crystal platelets. From one platelet with orientation $\vec{\alpha} = (010)$ it is possible to determine the four constants d_{21} , d_{22} , d_{23} and d_{25} , but for the remaining four constants d_{14} , d_{16} , d_{34} and d_{36} one crystal plate each is required. If the platelet with orientation $\vec{\alpha} = (010)$ has 3 side faces corresponding to 3 sets of non-equivalent Miller indices $h0\ell$ measurement of the longitudinal effect gives d_{22} , and of the transverse effect perpendicular to each of the 3 side faces gives 3 linear combinations each of the constants d_{21} , d_{23} and d_{25} . Of the remaining four measurements three may be made by using the longitudinal effect and give (if the above mentioned constants d_{21} , d_{22} , d_{23} and d_{25} have been determined independently) the constants d_{16} , d_{34} , $d_{14} + d_{36}$. In order to determine the constants d_{14} and d_{36} individually, one additional measurement based on the transverse effect is required.

For the determination of the 10 independent constants of class $C_s(m)$ 9 platelets with different orientations are required. While the platelet with $\vec{\alpha} = (100)$ permits to determine d_{11} through the longitudinal effect, and d_{12} through the transverse effect, the remaining 8 constants require for their determination one platelet each. While 5 linear combinations of

these constants (d_{26} , $d_{13} + d_{35}$, $d_{31} + d_{15}$, $d_{32} + d_{34}$, d_{33}) may be determined from the longitudinal effect, the remaining three independent measurements must be based on the transverse effect.

As shown by the data in Table 2 the 3 independent piezoelectric constants of class 222 have to be determined from the transverse effect by using 3 different crystal platelets with faces normal to the 3 coordinate axes, respectively. The longitudinal effect on a platelet with a pair of general (hkl) faces permits an independent measurement of the sum $d_{14} + d_{25} + d_{36}$.

The determination of the 5 independent constants for class $mm2(C_{2v})$ is illustrated below with the aid of a numerical example.

The discussion of Tables 3 to 6 for the remaining crystal classes proceeds along the same lines as above and need not be explicitly presented here.

3.6 Numerical Example

In order to illustrate and facilitate the use of Tables 1 to 6 the expressions for L and T required for the determination of the 5 independent constants of Bi_3TiNbO_9 (crystal class $mm2$) will be given here. The crystal structure of Bi_3TiNbO_9 has been refined from x-ray and neutron diffraction data by Wolfe, Newnham, Smith and Kay [1971]. These authors list the observed and calculated absolute values of the structure factors of a large number of non-equivalent reflections, from which suitable high intensity reflections can be selected.

According to Table 2 the 3 constants d_{31} , d_{32} and d_{33} can be determined from one platelet with a pair of electroded (001) faces, if the longitudinal effect is measured by Bragg reflection on the (001) face, resulting in d_{33} , and if the transverse effect is measured by Bragg reflection on two different

side faces of the type $(hk0)$, which gives two different linear combinations of d_{31} and d_{32} . Based on the structure factors listed by Wolfe, Newnham, Smith and Kay [1971] we select the three reflections 0010 , 040 , and 400 . The corresponding face normals \vec{N} are $(0,0,1)$, $(0,1,0)$ and $(1,0,0)$, respectively. From the lattice constants $a = 5.431 \text{ \AA}$, $b = 5.389 \text{ \AA}$ and $c = 25.050 \text{ \AA}$ given by Wolfe, Newnham, Smith and Kay [1971] the corresponding Bragg angles are calculated for CuK_α radiation and are listed in Table 7, together with the values of hkl , with the structure factors, and with the values of the platelet normal $\vec{\alpha}$ and the values \vec{N} of the three reflecting lattice planes. In Figure 1a the shape and orientation of the platelet with faces corresponding to these three normals and the corresponding Bragg angles θ_1 , θ_2 and θ_3 are illustrated schematically. Also listed in Table 7 are the corresponding values of L and T obtained from the last column of Table 2. According to equation (13) these quantities are equal to the electric field coefficient $-\cot \theta_i (\partial \theta_i / \partial E)$ ($i = 1, 2, 3$) of the associated Bragg angle. Denoting the experimental values of the electric field coefficient by M_i ($i = 1, 2, 3$) the three piezoelectric constants d_{33} , d_{32} and d_{31} are then given by the first three equalities listed in the last column of Table 7. According to Table 2 the remaining two constants d_{15} and d_{24} have to be determined from the transverse piezoelectric effect on two different platelets with side faces $(h0\ell)$ and $(0k\ell)$, with the corresponding normals of the side faces $(\xi 0 \zeta)$ and $(0 \eta \zeta)$, respectively, and with normals $(\bar{\zeta} 0 \xi)$ and $(0 \bar{\zeta} \eta)$ of the electroded main faces. In the fifth column of Table 2 the components $(\xi \eta \zeta)$ of these two normals are expressed in terms of the hkl values. On the basis of the structure factors listed by Wolfe, Newnham, Smith and Kay [1971] we select the reflections 0210 and 2010 . In Table 7 their structure factors, the normals \vec{N} of the side faces and the normals $\vec{\alpha}$ of the electroded main faces as calculated from columns 2, 4 and 5 of Table 2 are listed

Table 7. Miller indices hkl , calculated structure factors $|F_c|$ (in units given by Wolfe, Newham, Smith and Kay [1971]), face normals \vec{N} of crystal platelets representing reflecting lattice planes, face normals $\vec{\alpha}$ of electroded crystal platelet surfaces, representing direction of electric field \vec{E} , label i denoting six different experimental configurations, Bragg angle θ_i for $\text{CuK}\alpha$, type of piezoelectric effect (L = longitudinal, T = transverse), and LHS and RHS of equ. (12), consisting of electric field coefficients $M_i = -\cot \theta_i (\partial \theta_i / \partial E)$ (to be determined experimentally) and of linear combination $\alpha_{r i j}^N d_{r i j}$ of piezoelectric constants for $\text{Bi}_3\text{TiNbO}_9$, as obtained from entries of Table 2 for crystal class $\text{mm}2(C_{2v})$.

hkl	$ F_c $	$\vec{N} = (N_1, N_2, N_3)$	$\vec{\alpha} = (\alpha_1, \alpha_2, \alpha_3)$	i	θ_i	Type	$-\cot \theta_i \left[\frac{\partial \theta_i}{\partial E} \right] = \alpha_{r i j}^N d_{r i j}$
0 0 10	836	(0,0,1)	(0,0,1)	1	17.909°	L	$M_1 = d_{33}$
0 4 0	683	(0,1,0)	(0,0,1)	2	34.873°	T	$M_2 = d_{32}$
4 0 0	668	(1,0,0)	(0,0,1)	3	34.565°	T	$M_3 = d_{31}$
0 2 10	785	(0,0.6809,0.7324)	(0,-0.7324,0.6809)	4	24.826°	T	$M_4 = 0.3157d_{32} + 0.3652(d_{33} - d_{24})$
2 0 10	796	(0.6780,0,0.7350)	(-0.7350,0,0.6780)	5	24.731°	T	$M_5 = 0.3117d_{31} + 0.3663(d_{33} - d_{15})$
2 2 10	633	(0.5598,0.5642,0.6069)	(0.5598,0.5642,0.6069)	6	30.445°	L	$M_6 = 0.1902(d_{31} + d_{15}) + 0.1932(d_{32} + d_{24}) + 0.2235d_{33}$

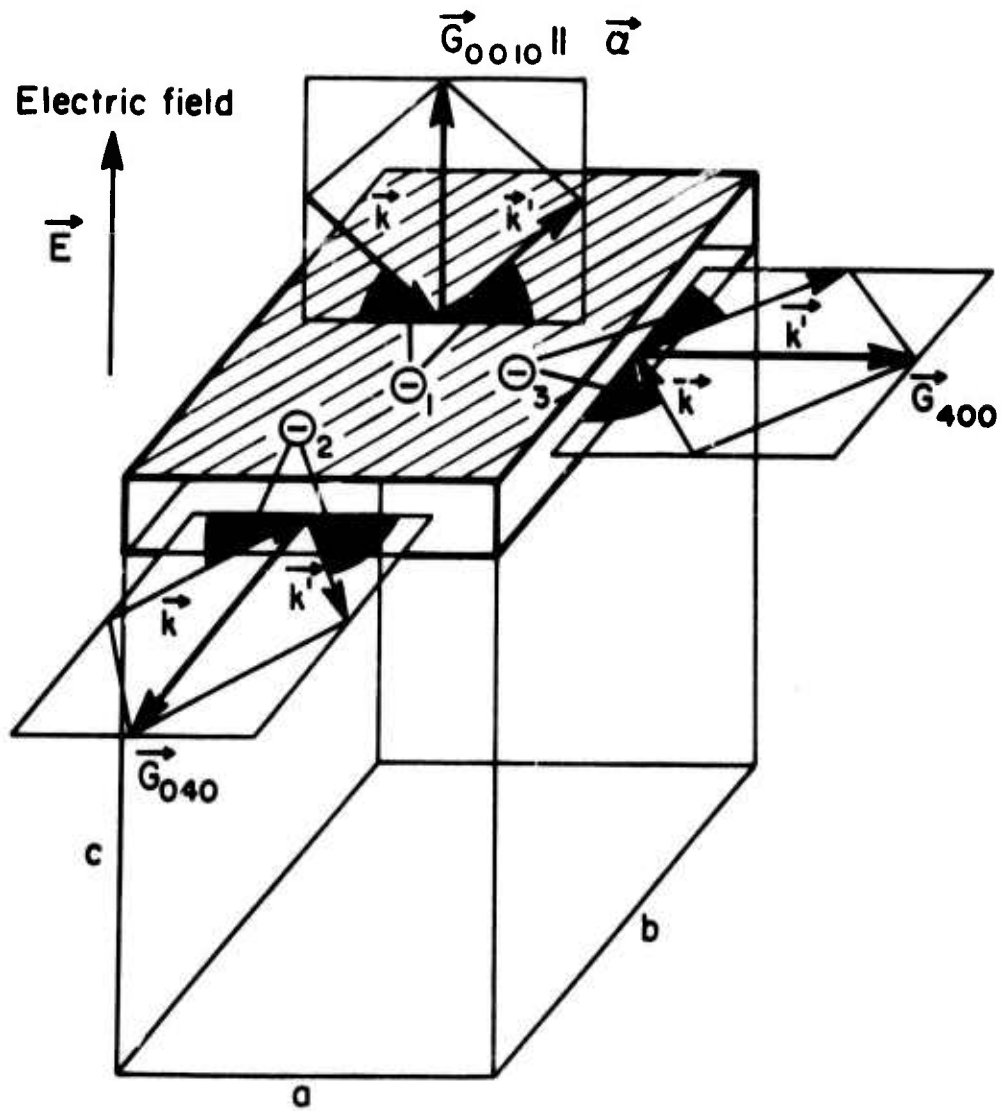


Figure 1a

Orientation of (001) platelet for determining electric field coefficient of θ_1 through longitudinal piezoelectric effect, and of θ_2 and θ_3 through transverse piezoelectric effect

together with the associated Bragg angles θ_4 and θ_5 . The orientation of these two platelets and the location of the two Bragg angles θ_4 and θ_5 is illustrated in Figures 1b and 1c. The last column of Table 7 gives the corresponding expressions for the quantity T obtained from the last column of Table 2. If experimental values of the electrical field coefficient $M_1 = -\cot \theta_1 (\partial \theta_1 / \partial E)$ are available for all five Bragg angles θ_i ($i = 1, 2, \dots, 5$) described, the equations given in the last column of Table 7 for M_1, M_2, \dots, M_5 represent 5 equations for the 5 unknown piezoelectric constants $d_{33}, d_{32}, d_{31}, d_{24}$ and d_{15} .

According to Table 2 an additional independent measurement of the longitudinal effect on a general (hkl) plane gives a linear combination of all 5 piezoelectric constants. Choosing for this purpose the $(2\ 2\ 10)$ reflection gives the entries listed on the last line of Table 7. The platelet orientation and the Bragg angle θ_6 are illustrated in Figure 1d. The six expressions for M_1, M_2, \dots, M_6 listed in Table 7 represent 6 equations for the 5 unknown piezoelectric constants. Their best values can be obtained from a standard simultaneous least squares fit.

For better accuracy additional platelets representing different values of $(0kl), (h0l)$ or (hkl) may be used ad libitum. It should be noted that for a given (hkl) face higher order and lower order reflections corresponding to different Bragg angles may be measured and should give the same value for the electric field coefficient. For example, the longitudinal field coefficient of all $(00l)$ reflections should be equal to d_{33} for any value of l . While the lower order reflections 002, 004, 006, 008 are of lower intensity than the 0010 reflection, the reflection 0 0 20 is also relatively strong and may be used to obtain an additional independent value for d_{33} .

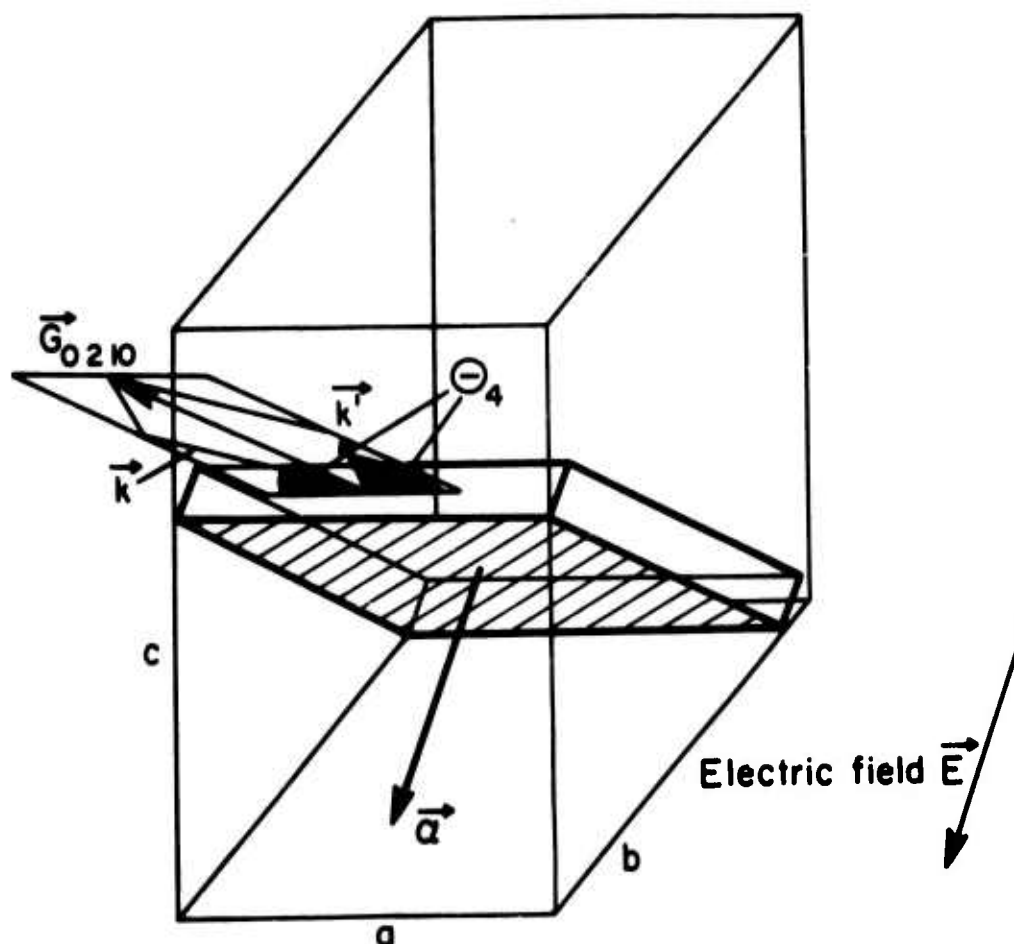


Figure 1b

Orientation of platelet for determining electric field
coefficient of O_4 through transverse piezoelectric effect

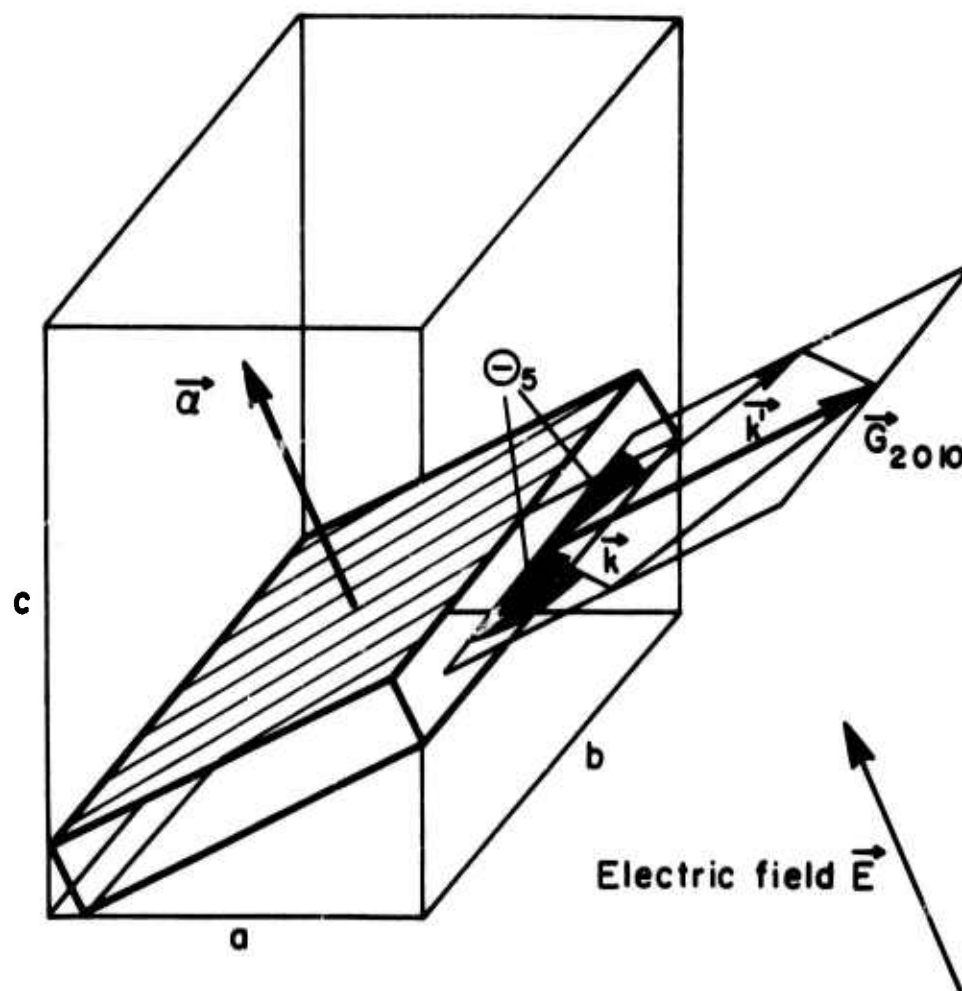


Figure 1c

Orientation of platelet for determining electric field
coefficient of θ_5 through transverse piezoelectric effect

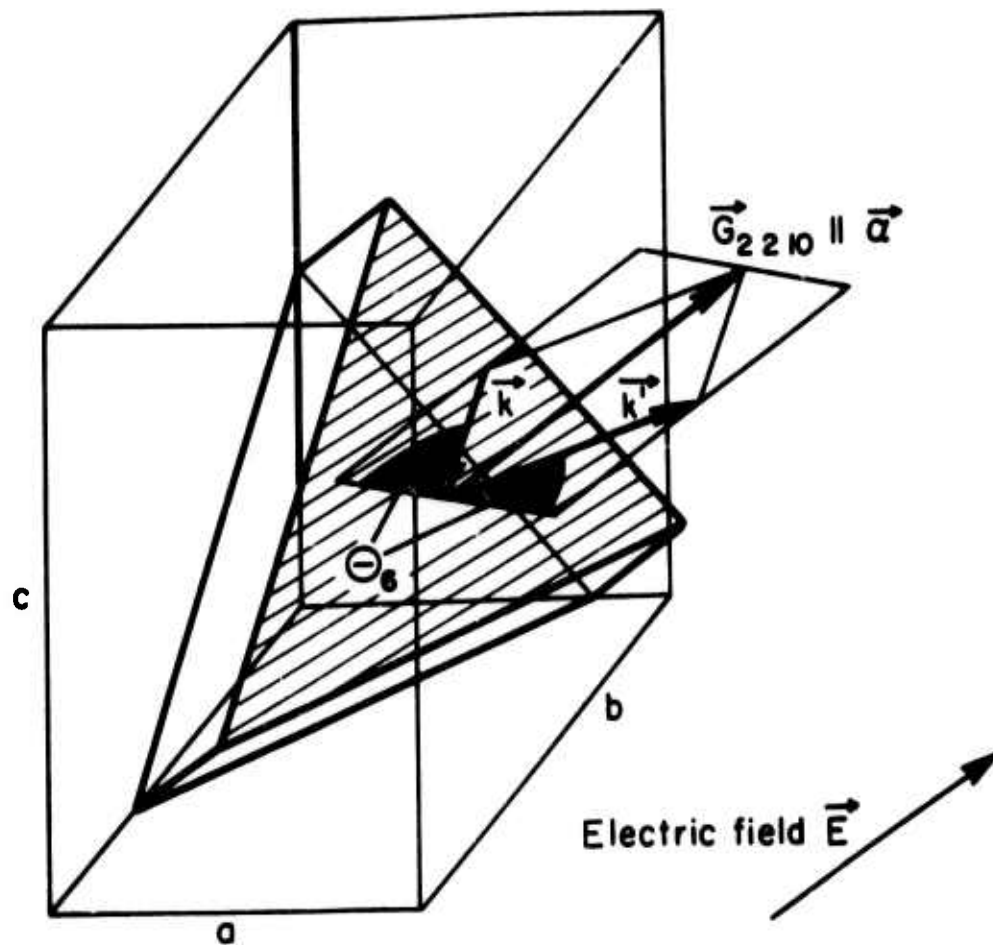


Figure 1d

Orientation of (115) platelet for determining electric field coefficient of Θ_6 through longitudinal piezoelectric effect

In order to reduce the experimental errors arising from the specimen orientation it appears more appropriate, however, to use additional crystal platelets representing different values of $(0kl)$, $(h0l)$, or (hkl) , which would lead to different numerical coefficients of the piezoelectric constants in the equations for M_4 , M_5 and M_6 , respectively.

4. Elastic and Thermoelastic Properties of Lead Potassium Niobate, $Pb_2KNb_5O_{15}$

Lead potassium niobate, $Pb_2KNb_5O_{15}$, occurs in the tungsten bronze structure and has electromechanical coupling factors up to 73 percent (Yamada, 1973). Since Yamada (1973) also reported that the temperature coefficients of the fundamental resonance frequencies of crystal plates cut along different directions have different signs, one may expect the temperature coefficient to vanish for intermediate directions. Provided that crystals of sufficient quality can be prepared, so as to reduce the ultrasonic attenuation to the intrinsic limit corresponding to anharmonic phonon-phonon interactions, and provided this limit is sufficiently low so as to be comparable to ultrasonic losses in α -quartz, lead potassium niobate would be a superior substitute for α -quartz in SAW devices. As reported above in section 2.3, our crystal growth efforts on this material met with considerable difficulties, but we did succeed in obtaining several small pieces which appear to be predominantly of single domain type. In the following we report our preliminary data on the elastic and thermoelastic properties and compare the results with those recently published by Nakano and Yamada (1975) and Yamada (1975).

$Pb_2KNb_5O_{15}$ belongs to the orthorhombic crystal class $mm2$ and is ferroelectric, with the spontaneous polarization along the b axis. The Curie temperature is $450^\circ C$ (Nakano and Yamada, 1975).

In Table 8 the three lattice parameters and their associated linear thermal expansion coefficients are listed. Based on the present x-ray results

Table 8. Lattice parameters (\AA) and linear thermal expansion coefficients ($10^{-5}(\text{°C})^{-1}$) of $\text{Pb}_2\text{KNb}_5\text{O}_{15}$ at 20°C .

L		a	b	c
L	Present	17.772	17.972	7.830
	Yamada*	17.78	18.05	3.917
$\frac{1}{L} \left(\frac{\partial L}{\partial T} \right)$	Present	3.09	1.06	3.77
	Yamada†	1.4	-0.3	1.7

* T. Yamada, Appl. Phys. Lett. 23, 213 (1973)

† T. Yamada, J. Appl. Phys. 46, 2361 (1975)

and lattice constant data for lead niobate, our lattice parameter c is twice that of Yamada's (1973) value. While the lattice constants agree rather well, the thermal expansion coefficients differ substantially; along the b axis even the sign is different. Although different experimental techniques were used (x-rays in the present work and a dilatometric technique by Nakano and Yamada (1975)) the differences cannot be attributed to this alone, and are more likely to point to differences in composition, structure or degree of disorder.

The calculated and measured density values in Table 9 show rather small differences between Yamada's and the present results, perhaps too small to point toward substantial compositional or structural differences. However, in order to explore the effect of ordering phenomena on property differences, a considerable amount of further work on possible correlations between

Table 9. Density values (in g/cm³) of Pb₂KNb₅O₁₅

	Calculated (X-Ray)	Measured
Present	6.15	6.23
Yamada*	6.12	6.14

*Yamada, Appl. Phys. Lett. 23, 213 (1973)

thermal history of the samples, their relative x-ray intensities and their elastic and thermoelastic properties is required. Since the measured densities are larger than the calculated values, the crystals used both by Yamada and in the present work may have had a small excess of lead.

In Table 10 the temperature coefficients of the transit times τ for longitudinal waves along the three crystallographic axes are compared with Yamada's (1975) values for the temperature coefficients of the corresponding principal resonance frequencies f . The relation between these two quantities is (Chang and Barsch, 1976)

$$\frac{1}{f} \left(\frac{\partial f}{\partial T} \right) = - \frac{1}{\tau} \left(\frac{\partial \tau}{\partial T} \right) - \frac{2kZ}{Z^2 - k^2(1 - k^2)} \left(\frac{\partial k}{\partial T} \right)$$

Here k denotes the electromechanical coupling factor, and Z the solution of the equation

$$\tan Z = Z/k^2$$

For small values of k and/or $(\partial k/\partial T)$ the temperature coefficients of f and τ should be numerically equal, but opposite in sign. According to Yamada (1975) the X- and Y-cut specimens have zero or small values of k for longitudinal waves, respectively, so that, unless $(\partial k/\partial T)$ is excessively large,

Table 10. Temperature coefficients of transit time for longitudinal waves, $(1/\tau)(\partial\tau/\partial T)$, and of fundamental resonance frequency, $(1/f)(\partial f/\partial T)$, (both in $10^{-6}(\text{°C})^{-1}$) for X, Y and Z cut of $\text{Pb}_2\text{KNb}_5\text{O}_{15}$ at 25°C.

	X-cut (\perp c-axis)	Y-cut (\perp a-axis)	Z-cut (\perp b-axis)
$(1/\tau)(\partial\tau/\partial T)$ (Present Work)	-3.03	84.00	74.82
$(1/f)(\partial f/\partial T)$ (Yamada*)	200	25	-30

*T. Yamada, J. Appl. Phys. 46, 2894 (1975)

$(1/\tau)(\partial\tau/\partial T) \approx -(1/f)(\partial f/\partial T)$. The data in Table 10 indicate that this relation does not at all hold. Again, this may be attributed to differences in composition, structure or degree of order.

The orientation of the cartesian x, y and z-coordinate axes along the crystallographic c, a and b-axes, respectively, follows the convention of Yamada (1975). These directions were determined optically by means of the quartz wedge method (see, e.g. Hartshorne and Stuart, 1964). In this manner a value of $\Delta n = n_a - n_b = 0.064$ for the difference of the refractive indices along the a and b axes was determined at 300°K, as compared with a value of $\Delta n = 0.055$ given by Nakano and Yamada (1975). The a and b axes can be distinguished on the basis of the sign of Δn and the fact that according to Nakano and Yamada (1976) the a-axis is the slow, and the b-axis the fast direction.

In Table 11 the on-diagonal elastic constants and their temperature coefficients are listed. The assignment of the coordinate axes follows Yamada (1975), that is $X||c$, $Y||a$, and $Z||b$. Except for c_{55} considerable differences in the elastic constants of Yamada and the present data occur. No other explanation except the above mentioned conjecture about differences in the nature of the sample can be offered.

It should be noted here that the as-grown boules obtained by us are of considerably higher quality than those of Nakano and Yamada (1975). Whereas the specimen on which the above elastic data were obtained do not show a significant amount of elastic twinning under a polarizing microscope (i.e. 90° domains for the spontaneous polarization $P_S||b$ -axis, or presence of domains with their a and b axes interchanged) the specimen obtained by Nakano and Yamada (1975) were thoroughly twinned and had to be de-twinned by strain annealing in an electric field. It is conceivable that by this procedure residual strains are introduced which could affect the elastic constant data.

Although the specimen used in the present investigations were virtually free of elastic twins, the presence of electrical twins (i.e. 180° domains for the spontaneous polarization) cannot be ruled out, since this type of twin cannot be detected under a polarizing microscope. In such twins all five piezoelectric constants of the class $mm2$ (that is, e_{15} , e_{24} , e_{31} , e_{32} , e_{33}) show opposite signs. However, since the piezoelectric stiffening term in the Kristoffel tensor depends only on the square of the piezoelectric constants the results for the elastic constants are not affected by the presence of 180° domains.

According to Table 11 the temperature coefficient of c_{11} is positive, so that one may expect temperature compensated cuts to exist for longitudinal waves along a direction close to the X -direction (c -axis). Unfortunately, this is not where the

Table 11. Adiabatic on-diagonal elastic constants $c_{\mu\nu}^D$ (10^{12} dynes/cm²), and their isobaric temperature derivatives $(\partial c_{\mu\nu}^D / T)_p$ (10^7 dynes/cm²) for $\text{Pb}_2\text{KNb}_5\text{O}_{15}$ at 25 C

$\mu\nu$		11	22	33	44	55*	66
$c_{\mu\nu}^D$	Present	1.46	1.03	1.45	.450	.600	
	Yamada	1.66	1.63	1.91	0.66	0.57	0.63
$\left(\frac{c_{\mu\nu}^D}{\partial T} \right)_p$	Present	+.465	-18.39	-29.49	-2.83	-5.50	

*This constant could not be measured since with the presently available crystal no echoes of the ultrasonic signal could be received.

†T. Yamada, J. Appl. Phys. 46, 2894 (1975)

electromechanical coupling factor reaches its maximum (Yamada, 1975). However, for the exact determination of the orientation of temperature compensated cuts for bulk or surface waves accurate values of all elastic, dielectric and piezoelectric constants and their temperature derivatives are needed. It is conceivable that the electromechanical coupling factor for these directions turns out to be larger than for α -quartz and α -berlinite (Chang and Barsch, 1976).

Our crystal growth efforts to obtain still larger single crystals required for the measurement of the remaining elastic and thermoelastic constants, and for the independent measurement of the dielectric and piezoelectric constants are being continued.

5. References

- BHALLA, A.S., BOSE, D.N., WHITE, E.W. and CROSS, L.E. (1971). phys. stat. sol. (a) 7, 335-339.
- BARSCH, G.R. and NEWNHAM, R.E. (1975). Piezoelectric Materials with Positive Elastic Constant Temperature Coefficients. AFCPL-TR-75-0163; Final Report on Contract No. 19628-73C-0108.
- CHANG, Z.P. and BARSCH, G.R. (1976). Elastic Constants and Thermal Expansion of Berlinite, IEEE Proc. Sonics Ultrasonics SU-23, 127-135.
- HARTSHORNE, N.H. and STUART, A. (1964). Practical Optical Crystallography, p. 189 ff, Edward Arnold Ltd., London.
- International Tables for X-ray Crystallography (1959). Vol. II, p. 106. Published for The International Union of Crystallography by The Kynoch Press, Birmingham, England.
- "IRE Standards on Piezoelectric Crystals, 1949" (1949). Proc. IRE 37, 1378-1395.
- MASON, W.P. (1950). Piezoelectric Crystals and Their Application to Ultrasonics, D. van Nostrand Co., Inc., New York, N.Y.
- NAKANO, J. and YAMADA, T. (1975). J. Appl. Phys. 46, 2361-2365.
- NYE, J.F. (1957). Physical Properties of Crystals, Clarendon Press, Oxford.
- WOLFE, R.W., NEWNHAM, R.E., SMITH, D. K. and KAY, M.I. (1971). Ferroelectrics 3, 1-7.
- YAMADA, T. (1973). Appl. Phys. Lett. 23, 213-214.
- YAMADA, T. (1975). J. Appl. Phys. 46, 2894-2898.

MISSION of Rome Air Development Center

RADC plans and conducts research, exploratory and advanced development programs in command, control, and communications (C³) activities, and in the C³ areas of information sciences and intelligence. The principal technical mission areas are communications, electromagnetic guidance and control, surveillance of ground and aerospace objects, intelligence data collection and handling, information system technology, ionospheric propagation, solid state sciences, microwave physics and electronic reliability, maintainability and compatibility.



Printed by
United States Air Force
Hanscom AFB, Mass. 01731